Energy Reports 14 (2025) 1020–1042

Contents lists available at ScienceDirect

Energy Reports

journal homepage: www.elsevier.com/locate/egyr

Research paper

Performance evaluation of photovoltaic self-consumption systems on industrial rooftops under continental Mediterranean climate conditions with multi-string inverter topology

J.L. Sánchez-Jiménez [a,b,d], G. Jiménez-Castillo [c,d,*], C. Rus-Casas [a,d], A.J. Martínez-Calahorro [a,b], F.J. Muñoz-Rodriguez [a,d]

[a] Department of Electronic and Automatic Engineering, University of Jaén, Jaén, Spain
[b] MarwenLab, Marwen, GEOLIT Science and Technology Park, Mengíbar, Jaén, Spain
[c] Department of Electrical Engineering, University of Jaen, Jaen, Spain
[d] Centre for Advanced Studies in Earth Sciences, Energy and Environment, University of Jaen, Jaen, Spain

ARTICLE INFO

Keywords:
Photovoltaic industrial rooftop
Self-consumption
Electricity energy
Performance analysis

ABSTRACT

This study analyses the performance and grid integration of seven photovoltaic self-consumption systems installed on industrial rooftops under real operating conditions. The analysed systems feature different orientations and peak power capacities, allowing to evaluate their behaviour through different indices and metrics proposed in the IEC 61724 and the literature, such as the Performance Ratio (PR), Final Yield (Y_f) or Capacity Utilisation Factor (CUF), among others. Additionally, the interaction of these systems with the load and the electrical grid is examined and proposed, providing a better view of their operation. The results reveal that, although most systems operate close to expectations, with PR, Y_f and CUF annual averages of 0.81, 1555.51 h/y and 0.19 respectively, factors such as partial shading, capture losses, and inverter configurations without grid injection affect their efficiency. The proposed Equivalent Capacity Utilisation Yield (Y_L), Load Ratio Yield (Y_{GL}), Load Ratio To Grid Yield ($Y_{GL,TG}$) and Load Ratio From Grid Yield ($Y_{GL,FG}$) are introduced to characterise the interaction between local demand and electrical grid constraints, providing a comprehensive assessment of system performance and grid use. A reduction in the full-load equivalent hours during which the interconnection node operates at its nominal capacity is observed following the integration of rooftop photovoltaic systems, as the values of Y_{GL} are consistently lower than those of Y_L. The results also indicate that the indices and metrics proposed in the literature, together with real data monitoring, are effective tools for evaluating the performance of photovoltaic systems and optimising their integration into electrical grids.

Introduction

Renewable energy is expected to surpass coal as the primary energy source by 2025 and together with nuclear energy, are projected to account for 46 % of global electricity generation by 2026 (International Energy Agency, 2024a); furthermore, photovoltaic (PV) solar and wind power are anticipated to lead capacity growth, reaching a 30 % share by 2030 and approximately 70 % of additional installed capacity by 2050 (International Energy Agency, 2023).

In 2023, global PV capacity reached 1.6 TW, with 407.3 GW of newly installed systems, 45 % of which were deployed on rooftops, both residential and industrial (International Energy Agency, 2024b). In Spain, throughout 2023, 1943 MW of self-consumption rooftop systems were installed, 76 % of which were in the residential and industrial sector, with target capacity of 76 GW by 2030 (SolarPower Europe, 2023; APPA Renovables, 2024). The deployment of PV systems on industrial rooftops has consolidated as a strategy to accelerate the energy transition, favoured by cost reductions and climate policies aiming to reduce emissions and strengthen energy security. This solution enables the utilisation of underutilised surfaces for renewable generation, optimising existing infrastructure, minimising the environmental impact.

The existing literature on the operational analysis of PV systems on industrial rooftops, as well as on the operation and maintenance (O&M) activities for these systems, is relatively recent. The majority of scientific

* Correspondence to: Departamento de Ingeniería Eléctrica, Edificio A3, dependencia 231 Campus Las Lagunillas s/n. 23071, Jaén, Spain.
E-mail address: gjimenez@ujaen.es (G. Jiménez-Castillo).

https://doi.org/10.1016/j.egyr.2025.06.047
Received 21 March 2025; Received in revised form 20 June 2025; Accepted 26 June 2025
Available online 18 July 2025

work focuses on large-scale PV plants (Santiago et al., 2018; Fuster-Palop et al., 2022; Montes et al., 2022). Studies on PV systems on industrial rooftops are scarce and have preliminary focused on their self-consumption potential (Martinez Calahorro et al., 2020; Jiménez-Castillo et al., 2023). These PV systems present a specific operational challenges that require further research to optimise their O&M (APPA Renovables, 2022).

Performance analysis of industrial rooftop PV systems may present additional complexities compared from those of residential, commercial buildings or utility-scale plants due to intrinsic factors. These include architectural constraints such as smaller roof slopes (typically between 5° and 15° in Spain) that may not be optimal for solar capture and distinct load-bearing designs. The losses of incident radiation due to not using the optimal tilt and orientation in the location of PV systems could reach 40 % in Spain (González-González et al., 2022). Although optimising azimuth and tilt angles could offer certain benefits from an energy efficiency standpoint, coplanar mounting remains widely adopted on industrial rooftops. This preference is due to its advantages, such as reduced costs, structural simplicity, lighter weight, visual impact and lower wind loads (Perdigones et al., 2023). An optimal azimuth and tilt angle for one industry may be ineffective or unsuitable for another, and could vary significantly depending on the load profile of each industry (Litjens et al., 2017).

Nevertheless, using industrial rooftops for PV systems presents a series of challenges not commonly encountered in large-scale solar farms. One key issue is the impact on the local microclimate: rooftop PV modules tend to increase module and surface temperatures, by several degrees, due to reduced natural ventilation beneath them, which in turn leads to higher cell temperatures and decreased performance (Fassbender et al., 2024). In addition, the presence of auxiliary structures or nearby buildings can generate persistent micro shadowing, which reduces the effective irradiance and, consequently, the output power (Lee et al., 2023).

Additionally, industrial rooftops are especially susceptible to soiling, which not only obstructs sunlight but also impairs thermal regulation. Dust accumulation could intensify module heating, leading to elevated cell temperatures, decreased performance and accelerated degradation of the panels (Borah et al., 2023). Other operational and environmental challenges specific to industrial settings include: increased maintenance complexity due to restricted access in buildings where electricity generation is not the primary activity; potential induction of specific microclimatic conditions caused by vapor emissions or other industrial gases; possible injection of harmonics into the electrical grid by industrial equipment; and difficulties in monitoring the PV system, often limited by space availability and the prioritisation of industrial operations.

Moreover, industrial buildings present significantly different energy consumption profiles, characterised by peak load demands, high energy intensity and high requirements for system reliability and operational flexibility. Ensuring a reliable energy supply while integrating PV systems requires advanced control strategies and modelling tools to manage production uncertainties (Polleux et al., 2022). Seasonality also strongly conditions the optimal size of industrial PV systems, the return on the investment and the potential savings (García et al., 2023). These peculiarities are what lead us to focus the performance analysis on industrial rooftops PV systems.

To quantify and analyse the performance of PV systems, the IEC 61724 standard establishes a standardised methodology (ISO/IEC, 2022, 2016a, 2016b). This standard defines a set of performance metrics and indices, including the final yield (Y_f), performance ratio (PR), conversion efficiencies and capacity utilisation factor (CUF). While performance indices enable intrinsic analysis of a specific installation, the metrics also facilitate comparisons between different systems, providing a framework for assessing whether they operate similarly under comparable conditions. This standard defines the variables to be measured (e.g., irradiance, temperature), the required sensors (type, accuracy, etc.), their installation (location, alignment, etc.), recalibration requirements or maintenance procedures. It also outlines measurement methodologies, data processing techniques, and the key parameters that should be calculated.

However, this standard focuses exclusively on the characterisation of the PV system, without considering how certain performance parameters may be influenced by the interaction with the energy consumption patterns of industrial processes. For instance, limitations at the grid connection node may prevent the inverter from operating at its maximum efficiency, directly affecting metrics such as the PR or CUF. Likewise, IEC 61724 does not incorporate indicators that allow assessment of the destination of the energy generated *in situ* specifically, the share self-consumed by the industrial facility versus the portion injected into the electrical grid. Nor does it provide parameters to analyse energy exchange flows with the electrical grid or to assess the utilisation level of the connection node relative to its design capacity, which is particularly relevant in contexts where the electrical infrastructure is constrained by other industrial loads.

Therefore, the main objective of this study is to evaluate and apply the performance metrics defined in current standards, as well as those widely recognised in the scientific literature, to analyse the behaviour of self-consumption PV systems installed in industrial environments. The analysis is based on monitored data from real systems with multi-string inverter topology, located in Mediterranean continental climate regions. Through this empirical approach, the operational performance of these systems under representative conditions is characterised, considering both electrical parameters and the environmental and operational constraints of the site. In addition to the analysis using standard indicators such as the PR and Y_f, this study also examines the suitability of such metrics in complex industrial contexts, identifying possible limitations or critical factors that are not currently accounted for but could significantly impact energy production and overall system performance. In this regard, the conventional evaluation framework is complemented with additional metrics that quantify the share of generated energy allocated to industrial self-consumption versus that exported to the utility grid. Furthermore, metrics are proposed to assess the degree of utilisation of the grid connection node relative to its nominal capacity, an essential factor for evaluating system scalability in terms of electrical infrastructure. This extended approach aims to provide a more comprehensive technical basis for optimising the design, sizing, and operation of future installations.

To address this study, the paper is structured as follows: after the introduction, which establishes the study's context, the second section presents a brief literature review, analysing key performance metrics of PV systems, their performance across different climates, and technologies related to modules and inverters. The third section details the case studies analysed, describing the industrial PV rooftops, the materials and the data used. The fourth section report the methodology and, subsequently, the results section presents the findings and the discussion section compares them with existing literature and analyses their implications. Finally, the conclusions summarise the study's contributions.

Literature review

This section presents a brief literature review regarding the metrics used for analysing the performance of PV self-consumption systems, including those established in regulatory standards and those proposed by Sandia and NREL laboratories. Additionally, other relevant metrics

identified in the literature are included, along with an analysis of their frequency of use in the reviewed scientific papers. Furthermore, the impact of PV module technology and inverter topology on the PR and Y_f is examined based on data reported by the scientific community.

Trends in photovoltaic systems performance metrics

The IEC 61724–1 standard defines multiple parameters for evaluating the performance of PV systems. These parameters characterise overall performance related to energy generation, solar resource availability and system losses, as summarised in Table 1. For their definitions and calculation methods, refer to the methodology section.

In addition to the parameters and metrics recommended by the standard, various institutions, such as the International Energy Agency (IEA) (Woyte et al., 2014) and the U.S. National Renewable Energy Laboratory (NREL) (Kurtz et al., 2013), have proposed complementary guidelines. NREL's proposed parameters closely align with those recommended by the IEC 61724 standard. In contrast, the IEA introduces two impact factors for performance analysis: the spectral mismatch factor (MM) and the spectral impact factor (SIF), with the latter directly depending on the former. The MM factor is based on the premise that instantaneous PV production can be modelled by scaling the incident irradiance with a mismatch factor. The SIF can then be applied as a linear scaling factor to the measured or calculated energy yield, accounting for the difference between the effective local mean spectrum and the AM1.5 reference spectrum (Woyte et al., 2014). It is important to note that both approaches primarily focus on large-scale plants. Some of the suggested parameters may be challenging to monitor in small- or medium-scale systems, such as those installed on commercial and industrial rooftops. This limitation constrains their direct applicability in smaller-scale contexts but does not preclude their potential usefulness as a reference for methodological adaptations.

Table A in appendix A presents an analysis of the performance metrics usage trends of PV systems studied in the literature. This analysis incorporates parameters established by IEC standards as well as newly developed metrics proposed by the scientific community. The PV plants examined are located across a wide range of geographical regions, with data collected over different time periods. The trend in the use of performance metrics has not been classified according to module and inverter technology. Table 2 provides a summary of the most relevant findings from this analysis. Each row represents a parameter, while the "n" column provides information on the frequency of occurrence of each parameter in the total of 106 articles analysed and "%" represents the prevalence of these parameters in the reviewed literature.

Table 1
Calculated parameters proposed by the IEC 61724–1 standard for the performance analysis of photovoltaic systems.

Parameter	Symbol	Unit
Irradiation		
In-plane irradiation	H_i	$kWh{\cdot}m^{-2}$
Electrical energy		
PV array output energy (DC)	E_A	kWh
Energy output from PV system (AC)	E_{out}	
Array power rating		
Array power rating (DC)	P_0	kW
Array power rating (AC)	$P_{0,CA}$	
Yields and yield losses		
PV array energy yield	Y_A	$kWh{\cdot}kW^{-1}$ or h
Final system yield	Y_f	
Reference yield	Y_r	
Array capture loss	L_c	
Balance of system (BOS) loss	L_{BOS}	
Performance ratio	PR	p.u.
Efficiencies		
Array efficiency	η_a	p.u.
System efficiency	η_f	
BOS efficiency	η_{BOS}	
Capacity		
Capacity utilisation factor	CUF	p.u.

Adapted from (ISO/IEC, (2022).

Table 2
Performance metrics of PV systems used in the scientific literature by frequency of use.

Parameter	n	%
Performance Ratio (PR)	103	97.17
Final yield (Y_f)	89	83.96
Capacity utilisation factor (CUF)	69	65.09
Reference yield (Y_r)	59	55.66
Array yield (Y_A)	51	48.11
Array capture loss (L_c)	48	45.28
System efficiency (n_{sys})	48	45.28
Balance of system loss (L_{BOS})	45	42.45
Array efficiency (n_a)	30	28.30
Inverter efficiency (n_{inv})	27	25.47
Cell temperature loss (L_T)	3	2.83
Performance Ratio corrected by temperature (PRT)	2	1.89
Balance of system efficiency (n_{BOS})	1	0.94
Total loss (L_t)	1	0.94

Out of a total of 106 studies providing performance data, the PR exhibits the highest frequency, being used in 97.17 % of the studies. It is closely followed by Y_f at 83.96 % and CUF at 65.09 %. Additionally, some parameters, such as Performance Ratio corrected by temperature (PRT) and Total loss (L_t), show low usage frequencies of 1.89 % and 0.94 %, respectively. This suggests that the scientific community has not widely reported results related to these parameters. On the other hand, energy losses occurring in different parts of the system, such as Array capture loss (L_c) and Balance of system loss (L_{BOS}), are used in more than 40 % of the analysed systems.

Yields and performance ratios of commissioned plants

The values of PR and Y_f reported in the studies analysed in the previous section have been examined, as shown in Fig. 1. The size of the array in a PV rooftop system can range from just a few square meters to several thousand, making the classification of these systems somewhat ambiguous. To ensure a consistent analysis of rooftop systems, the maximum installed capacity has been restricted to 1 MW, considering that large industrial facilities may have rooftop areas equivalent to this capacity. Among the 106 reviewed systems, 76 have a nominal power capacity below 1 MW. However, only 62 are rooftop systems.

The Y_f values are expressed in average hours per day (h/d), representing the time required for the PV field to operate at its nominal capacity to generate an amount of energy equivalent to the incident energy. The units used correspond to those most commonly reported in the reviewed studies. Similarly, PR values are presented as annual percentages.

Notably, 25 % of the PV plants exhibited a PR below 70 %. The observations reveal a variability in PR values ranging from 49 % to 94 %. Compared to large-scale PV plants, medium and small-scale systems show a dispersed distribution (Jianxun et al., 2023). This wide dispersion reflects the diversity of real-world operating conditions typical of medium and small-scale systems, which often face suboptimal orientations, partial shading, heterogeneous maintenance practices and variable inverter configurations. The Y_f values range from 1.6 to 5.3 h/d. Most of the reported studies analyse systems with installed capacities below 200 kW. At first sight, no significant correlation is observed between PR and Y_f concerning the installed capacity of the systems. There are cases where systems with similar installed capacities have different PR and Y_f values. This behaviour has been corroborated by other authors, who have stated that the PR of PV systems analysed across different regions does not show a correlation with latitude or installed

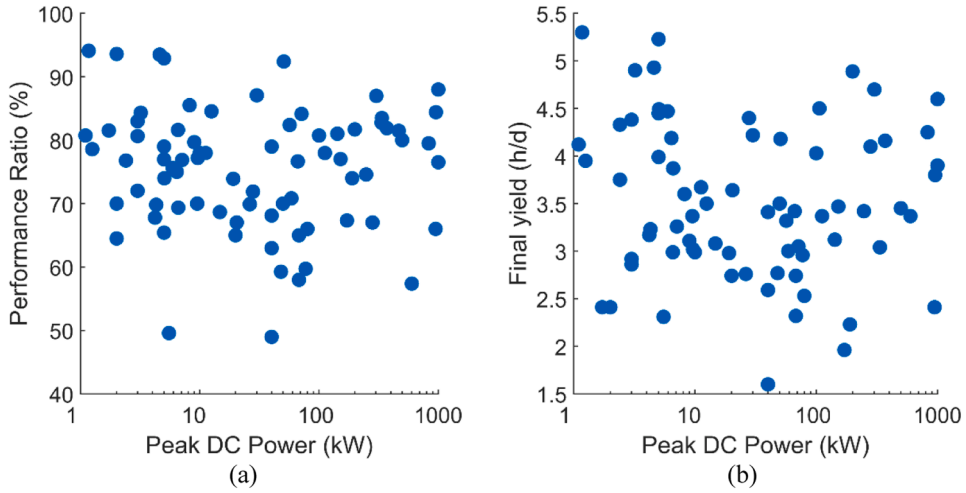

Fig. 1. Performance ratio and Final yield versus installed peak DC power in logarithmic scale for systems below 1 MW; (a) Performance ratio; (b) Final yield.

capacity (Schardt and te Heesen, 2021; Taylor et al., 2015).

Impact of module and inverter technology on performance metrics

The Y_f and lifespan of a PV system are determined by several factors, including the type of PV technology used, the type of inverter technology, meteorological conditions, the amount of solar radiation received, dust accumulation, ambient temperature, cell temperature, partial shading, module orientation and tilt, and geographical location (Farahmand et al., 2021).

The appropriate selection of module and inverter technology has a significant impact on maximising system efficiency and durability. Various PV technologies are commonly used in the market, including crystalline silicon (monocrystalline, m-Si; and polycrystalline, p-Si) and thin-film technologies such as amorphous silicon (a-Si), cadmium telluride (CdTe), copper indium selenide (CIS), and copper indium gallium selenide (CIGS). The literature includes several studies comparing the performance of different PV technologies. Atsu, Seres, and Farkas evaluated the performance of two PV technologies in grid-connected systems in Hungary (p-Si and a-Si). Their study concluded that p-Si technology achieved a higher PR than a-Si, with values of 77.2 % and 58.8 %, respectively (Atsu et al., 2021). Similarly, Bennouna et al. analysed energy production from different silicon-based PV technologies (m-Si, p-Si, and a-Si) under Moroccan climatic conditions (Bennouna et al., 2019). Their findings indicated that the performance of these silicon technologies varied significantly depending on location and environmental conditions, with polycrystalline silicon (p-Si) demonstrating superior performance compared to the others. Furthermore, Emziane and Al Ali evaluated four rooftop PV systems using monocrystalline and polycrystalline technologies (Emziane and Al Ali, 2015). Their analysis showed that polycrystalline technologies outperformed monocrystalline ones, with a PR of 80 % compared to 70 %. Although monocrystalline modules have higher efficiency, the authors attributed these results to differences in tilt angle, inverter type, and system efficiency.

Fig. 2 illustrates the performance of the most commonly used PV technologies as a function of rated peak power: monocrystalline silicon, polycrystalline silicon, and thin-film modules. PR values tend to cluster within a common range for all three technologies, typically between 65 % and 85 %. On average, these technologies achieve a PR of

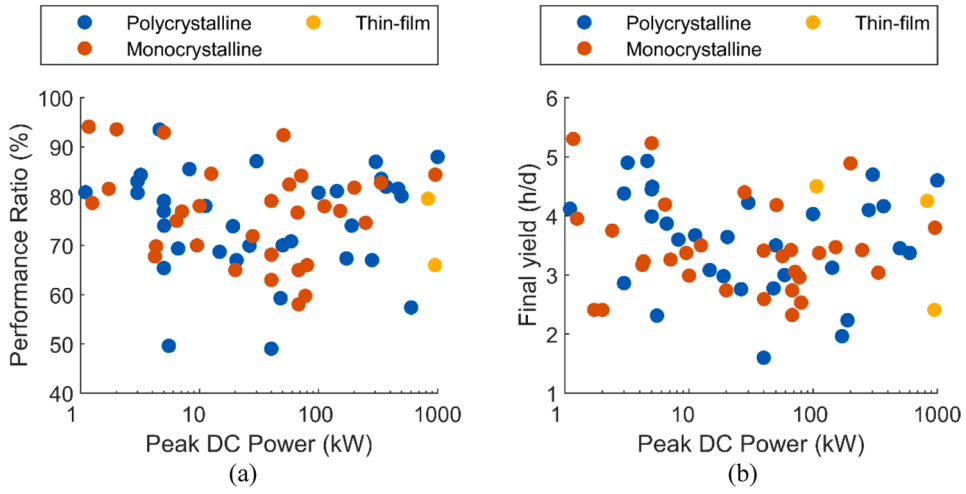

Fig. 2. Performance ratio and Final yield of PV systems below 1 MW versus installed peak power in kW and logarithmic scale for different module technologies; (a) Performance ratio; (b) Final yield.

approximately 75 % across various PV systems worldwide (Srivastava et al., 2020). Similarly, no predominant technology is observed in terms of Y_f when analysed comprehensively. Scientific studies indicate that, in real-world systems, there is no significant difference in PR and Y_f values among the three analysed technologies. In operational conditions, elements such as degradation losses, climatic variability and the management of operation and maintenance may have a comparable impact across different module technologies, ultimately homogenising their performance in terms of these metrics.

According to the module data sheets, monocrystalline technology shows higher efficiency compared to polycrystalline technology, as well as a lower annual degradation rate. However, based on the results, it is challenging to draw definitive conclusions regarding the PR, as it is influenced by multiple factors, as previously discussed. In most of the analysed studies, the commissioning date is not reported. This date could provide the service years of the plant and reduce the limitation to analyse degradation and performance and, consequently, may affect the PR. In this regard, future studies would greatly benefit from more detailed and comprehensive information provided by researchers.

Similarly, the selection of the inverter must consider its efficiency, compatibility with the direct current (DC) field, and compliance with alternating current (AC) electrical grid compatibility and safety requirements. The synergy between modules and inverters significantly influences the system's overall energy efficiency. Proper matching can minimise losses, thereby optimising performance and extending the system's lifespan. Inverter topologies include central inverters, single-MPPT, multi-MPPT, and micro-inverters, each offering different advantages depending on system design and operational conditions (Zeb et al., 2018; Puche et al., 2016), Fig. 3.

Central inverters use series-parallel PV module configurations but suffer from losses, complexity and limited modularity. Single-MPPT inverters, with one MPPT, offer better efficiency and shading tolerance. Multi-MPPT inverters improve modularity and control via individual DC-DC converters and multiple MPPTs. Modules inverters can eliminate mismatch losses and simplify installation, though they raise costs and system complexity. Fig. 4 illustrates the performance of the most widely used grid-connected PV inverter configurations based on installed capacity.

The scientific literature reports a higher number of systems using central inverters compared to other configurations. This is followed by the multi-MPPT configuration. Notably, systems employing this configuration often achieve higher PR and Y_f values than those using central inverters. Currently, multi-MPPT inverters are the most widely used topology in small-scale systems, as they offer higher system availability, reliability and energy efficiency (Motahhir et al., 2020). Additionally, micro-inverters can be deployed to associate each panel with its own DC/DC converter. This configuration significantly mitigates shading issues or panel failures, which in central inverter setups can lead to substantial energy losses (Lagarde et al., 2023). While multi-MPPT inverters and other decentralised configurations enhance energy harvesting under non-ideal conditions, their implementation is more common in small-scale rooftop systems than in utility-scale plants. Consequently, the performance of rooftop PV systems may differ from utility-scale installations due to specific design constraints and operational contexts.

These variations are primarily influenced by the technical and economic feasibility studies typically conducted for large-scale plants, as well as the diverse configurations available for rooftop systems. Table 3 presents the average daily Y_f values and PR of smaller rooftop grid-connected systems in Spain, along with details on the module and inverter technologies used.

It is observed that single-MPPT inverters shows a wide range of PR values, fluctuating between 49 % and 81 %, indicating that a consistently high performance has not been observed in the analysed systems. For instance, the 40.0 kW system reports a PR of 49 % and a Y_f of 1.60 h/d. Conversely, smaller systems, such as the 1.10 kW, achieve a PR of 81 % with a Y_f of 4.12 h/d, suggesting that single-MPPT inverters may be more suitable for low-power systems. On the other hand, central inverters, despite being suitable for managing large amounts of energy, their PR are low among the analysed technologies, with values of 58 % and 65 %. This trend is also reflected in the Y_f values, which vary between 2.32 h/d and 2.74 h/d, indicating lower energy efficiency compared to multi-MPPT and single-MPPT inverters.

Regarding multi-MPPT inverters, an analysed 3.0 kW system showed high PR and Y_f values of 83 % and 4.38 h/d, respectively. Similar results were observed in a year-long study of a 1.05 MW system distributed across five building rooftops and a parking structure, featuring 12 multi-string topology inverters, which achieved an average PR of 85 % and an average Y_f of 4.27 h/d (Muñoz-Rodríguez et al., 2025). This suggests that multi-MPPT inverters may effectively optimise energy capture in small-scale rooftop systems compared to other inverter technologies. Studies indicate that systems employing multi-MPPT inverters demonstrate higher performance, particularly during peak production periods (Díez-Mediavilla et al., 2014). Additionally, empirical tests suggest that

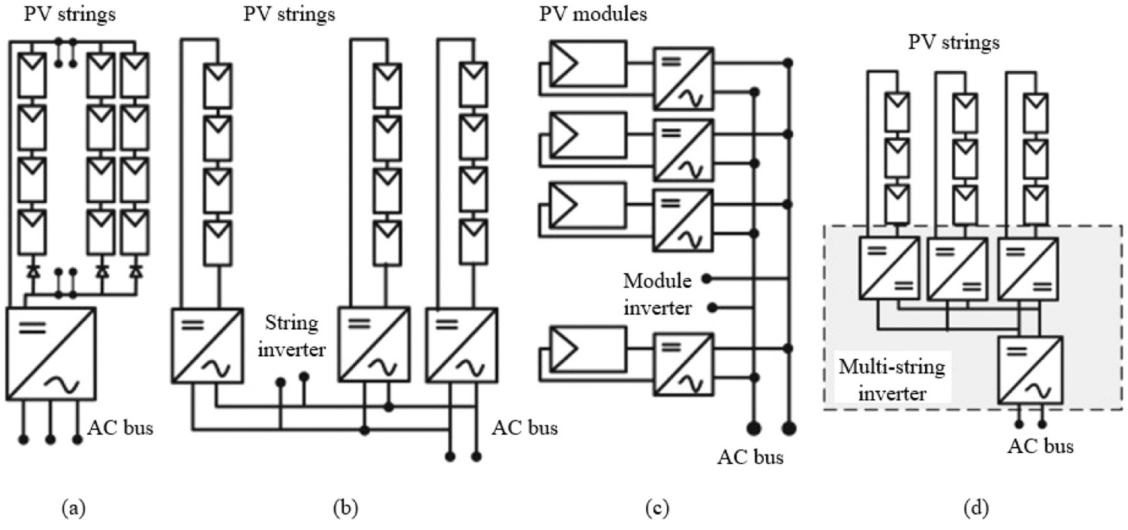

Fig. 3. Configurations of grid-connected PV inverters; (a) central; (b) single-MPPT; (c) micro-inverter; (d) multi-MPPT (Zeb et al., 2018).

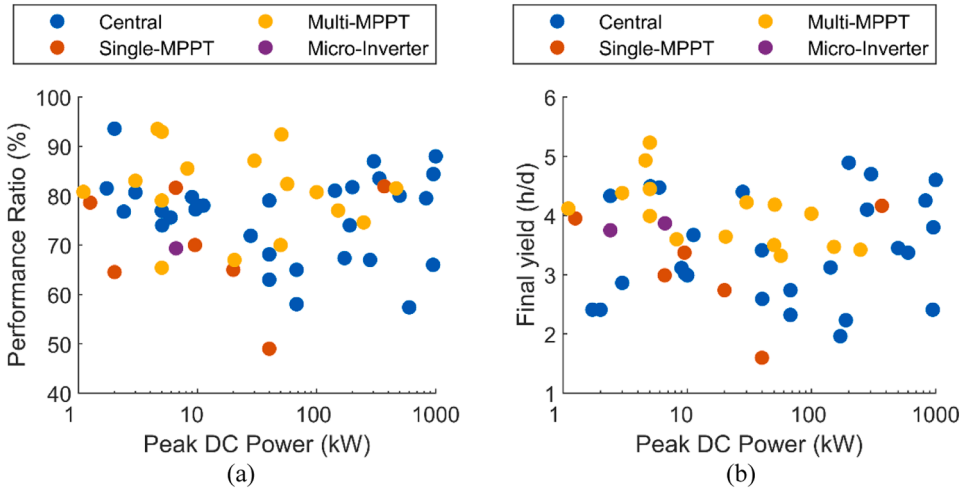

Fig. 4. Performance ratio and Final yield of PV systems below 1 MW versus installed peak power in kW and logarithmic scale for different inverter topology; (a) Performance ratio; (b) Final yield.

Table 3
Performance analysis of different PV rooftop systems in Spain.

Rated power (kWp)	Design	Module technology	Inverter technology	PR (%)	Y_f (h/d)	Ref.
1.17	On-Grid Rooftop	Monocrystalline	Micro-Inverter	94	5.30	(Piliougine et al., 2013)
1.25		Monocrystalline	Single-MPPT	79	3.95	(Guerra et al., 2017)
1.10		Polycrystalline	Single-MPPT	81	4.12	(Guerra et al., 2017)
2.00		-	Single-MPPT	64	-	(Sidrach-De-Cardona and López, 1998)
3.00		Polycrystalline	Multi-MPPT	83	4.38	(Muñoz-Rodríguez et al., 2023)
4.30		Monocrystalline	Single-MPPT	70	3.23	(De Miguel et al., 2002)
20.00		Monocrystalline	Single-MPPT	65	2.74	(Drif et al., 2007)
40.00		Polycrystalline	Single-MPPT	49	1.60	(Drif et al., 2007)
67.84		Monocrystalline	Central	65	2.74	(Drif et al., 2007)
67.84		Monocrystalline	Central	58	2.32	(Drif et al., 2007)

these inverters exhibit higher energy efficiency under partial shading conditions (Ali and Khan, 2020). While central inverters remain the most cost-effective option in the market, they have been associated with increased energy losses due to voltage mismatches between parallel-connected strings, as well as greater heating and diode failure rates (Dogga and Pathak, 2019; Zeb et al., 2018). Single-MPPT and multi-MPPT inverters have shown superior performance over central inverters in both shaded and non-shaded environments, yielding higher energy production and reduced costs under different climatic conditions (Desai et al., 2020). In this context, multi-MPPT inverters enhance renewable energy integration and emerge as a viable solution for rooftop PV systems (Ocampo et al., 2021).

Having identifying the most commonly used metrics in the performance analysis of PV systems, the following section will detail the application of these indices to the analysis of seven PV self-consumption systems on industrial rooftops under real operating conditions. In addition, the importance of module and inverter technology in the performance of these systems has been highlighted during the review, as well as the growing interest in the performance analysis of PV systems on industrial rooftops, facts that have motivated this research.

Cases studies and materials

This section describes the seven PV self-consumption systems installed on industrial rooftops used in this study. Additionally, it details the monitored data employed and the equipment used for data sampling. The systems have been monitored over one year of operation. Electrical parameters from both the direct current (DC) and alternating current (AC) sections, as well as environmental parameters, have been recorded. The measured parameters include in-plane irradiance, G_k, array voltage (DC), V_A, array current (DC), I_A, array power (DC), P_A, and output power (AC), P_{out}.

Regarding in-plane incident radiation and module temperature, the MET cell from Datasol is used. This electronic device enables the acquisition of solar radiation, module temperature, and ambient temperature. The MET radiation measurement includes module temperature compensation and operates within a range of 0–1400 $W{\cdot}m^{-2}$, with an uncertainty of ± 2.2 % and a resolution of $\leq 1\ W{\cdot}m^{-2}$. For electrical parameters, AC network measurements are performed using the DTSU666-H energy meter from Huawei in systems #01, #04, #05, #06, and #07, while plants #02 and #03 employ the UMG 103-CBM energy analyser from Janitza. On the DC side, electrical parameters are obtained from the internal monitoring system of the Huawei inverters. The monitoring system collects, visualises and stores data via a web server, enabling efficient data retrieval for detailed analysis or real-time supervision. Electrical and environmental parameters are recorded following the IEC 61724 standard, depending on the system size. The selected storage interval is five minutes, in accordance with the recommendations of the standard (ISO/IEC, 2022).

The seven systems analysed have a rated peak DC power (P_0) value of 54.39 kW (#01), 44.10 kW (#02), 37.24 kW (#03), 3.64 kW (#04), 16.20 kW (#05), 50.40 kW (#06), and 18.00 kW (#07). Table 4

Table 4
A Picture of the facilities used in the study, along with the technical specifications of the PV modules and inverters for the PV self-consumption systems.

		Technical specifications	
#01 Location Andalusia, Spain Commissioning date, 10/03/2022		P_0	54.39 kW
		No. PV modules	111
		Nominal PV module power	490
		No. Inverters	2
		Inverter model	30/20 KTL-M3
		Total strings	8
		Inverter 30 KTL-M3	5 strings
		MPPT1	1 string
		MPPT2	1 string
		MPPT3	1 string
		MPPT4	2 strings
		Inverter 20 KTL-M3	3 strings
		MPPT1	2 strings
		MPPT2	1 string
		Orientation	S – E – W
		South power	22.05 kW
		East power	17.64 kW
		West power	14.70 kW
		Tilt	10°
#02 Location Andalusia, Spain Commissioning date, 01/02/2022		P_0	44.10 kW
		No. PV modules	90
		Nominal PV module power	490
		No. Inverters	1
		Inverter model	40 KTL-M3
		Total strings	6
		MPPT1	2 strings
		MPPT2	1 string
		MPPT3	1 string
		MPPT4	2 strings
		Orientation	E – W
		East power	22.05 kW
		West power	22.05 kW
		Tilt	10°
#03 Location Andalusia, Spain Commissioning date, 14/01/2022		P_0	37.24 kW
		No. PV modules	76
		Nominal PV module power	490
		No. Inverters	1
		Inverter model	36 KTL-M3
		Total strings	6
		MPPT1	2 strings
		MPPT2	2 strings
		MPPT3	1 string
		MPPT4	1 string
		Orientation	S
		South power	37.24 kW
		Tilt	10°
#04 Location Andalusia, Spain Commissioning date, 21/02/2022		P_0	3.64 kW
		No. PV modules	8
		Nominal PV module power	455
		No. Inverters	1
		Inverter model	3 KTL-M1
		Total strings	1
		MPPT1	1 string
		Orientation	S
		South power	3.64 kW
		Tilt	12°
#05 Location Andalusia, Spain Commissioning date, 24/05/2022		P_0	16.20 kW
		No. PV modules	36
		Nominal PV module power	450
		No. Inverters	1
		Inverter model	15 KTL-M2
		Total strings	2
		MPPT1	2 strings
		MPPT2	0
		Orientation	E – W
		East power	8.10 kW

(*continued on next page*)

Table 4 (*continued*)

		Technical specifications	
		West power	8.10 kW
		Tilt	30°
#06 Location Andalusia, Spain Commissioning date, 12/12/2022		P_0	50.40 kW
		No. PV modules	112
		Nominal PV module power	450
		No. Inverters	1
		Inverter model	60 KTL-M0
		Total strings	7
		MPPT1	2 strings
		MPPT2	2 strings
		MPPT3	2 strings
		MPPT4	1 string
		MPPT5	0
		MPPT6	0
		Orientation	E – W
		East power	25.20 kW
		West power	25.20 kW
		Tilt	12°
#07 Location Andalusia, Spain Commissioning date, 17/02/2022		P_0	18.00 kW
		No. PV modules	40
		Nominal PV module power	450
		No. Inverters	1
		Inverter model	15 KTL-M2
		Total strings	2
		MPPT1	2 strings
		MPPT2	0
		Orientation	S
		South power	18.00 kW
		Tilt	15°

provides the geographical distribution of these industries, a visual representation of the PV self-consumption systems, and technical specifications related to modules, arrays, inverters, and orientations. In addition, the number of total strings of each industry array is shown, as well as the strings associated with each of the MPPT of the inverters.

Every system incorporates Huawei SUN2000 inverters, specifically designed for industrial applications in three-phase systems. These inverters have a European efficiency of 96.7 % for 3 kW units (#04), 98.3 % for 15 kW units (#05 and #07), 97.2 % for 20 kW units (#01), 98.4 % for 30 kW (#01), 36 kW (#03), and 40 kW (#02), and 98.5 % for 60 kW units (#06). According to the technical specifications, the MPPT inputs operate within a voltage range of 200 V to 1000 V.

During the analysis period, system #06 operated under two different inverter configurations regarding the injection of electrical energy into the grid. In January, February, and March, the inverter was set to prevent energy injection at the connection node between the industry and the public distribution grid. This configuration aimed to ensure that the power at the grid connection node remained balanced with the consumer demand, provided that internal consumption exceeded the measurement system's tolerance. This tolerance was calculated as the sum of the accuracy classes of the power measurement equipment and the class of the current transformer or sensor. For the remainder of the analysis period, both for system #06 and for the entire period of the other systems, the inverters were not configured to prevent energy injection into the grid. Therefore, they operated by searching the maximum power point.

The characteristics of these seven systems will allow the application of the performance metrics reviewed in the previous section, such as PR and Y_f, to analyse their behaviour.

Methodology

The first step involves processing and validating the data in accordance with the standard's recommendations. This includes analysing the data to identify outliers beyond acceptable operational ranges, values that remain constant over extended periods, gaps in records, and abrupt variations between consecutive points that lack justification, following the technical guidelines outlined in IEC 61724–1, 2 and 3 (ISO/IEC, 2022, 2016a, 2016b). Subsequently, parameters and metrics are computed as specified by the standard for different PV systems. The following formulations, characterised by summations, incorporate the temporal aspect, where τ_k represents the duration of the k-th recording interval within a defined reporting period τ. The summation symbol Σ_k denotes the sum of all recording intervals within the reporting period. For instance, τ_k may correspond to a day, a month, or a year, while k may be set at 1, 5, 15, or 60 min. It is important to note that in formulas where power quantities are multiplied by the recording interval τ_k, power should be expressed in kilowatts (kW) and the recording interval in hours (h), ensuring that the resulting energy is measured in kilowatt-hours (kWh).

The PV in-plane irradiation, denoted by H_i and measured in [kWh·m^{-2}], is determined by multiplying the sum of the irradiance values G_k by the recording interval τ_k:

$$H_i = \sum_k G_k \times \tau_k \tag{1}$$

When calculating the overall system irradiation, it has to be taken into account that there are PV arrays corresponding to each subsystem or PV roof with different tilt and orientation. In order to provide a proper analysis, a new weighted irradiation of the system in the plane, $H_{i,weighted}$, must be considered:

$$H_{i,weighted} = \frac{\sum_{j=1}^{p} H_{i,j} \cdot P_{0,sub,j}}{P_0} \tag{2}$$

$H_{i,j}$ corresponds to the in-plane irradiance of subsystem j, while p gives the total number of subsystems. P_0 is the rated power of the whole

PV system. $P_{0,sub,j}$ represents the rated power of subsystem j (Muñoz-Rodríguez et al., 2025).

The power output of the PV array, represented as the DC output power of the PV array and expressed in [kW], is calculated as follows:

$$E_A = \sum_k P_{A,\,k} \times \tau_k \tag{3}$$

The cumulative AC output power [kWh] of the PV system at the inverter output, called E_{out}, is calculated from the inverter output power, P_{out}, taking into account the recording interval τ_k:

$$E_{out} = \sum_k P_{out,\,k} \times \tau_k \tag{4}$$

Yields represent the ratio between an amount of energy and the rated array capacity (P_0), serving as an indicator of the actual array operation relative to its rated capacity. They are expressed in [kWh·kW^{-1}], where kWh in the numerator indicates the energy output and kW in the denominator indicates the rated power of the system.

The energy yield of the PV array (Y_A) is defined as the energy output (DC) per rated kilowatt (DC) of the installed PV array.

$$Y_A = E_A / P_0 \tag{5}$$

Where:

P_0: is the sum of the direct current (DC) power outputs generated by all installed PV modules, measured under standard test conditions and in the reference conditions for the rated power.

The final system yield, called Y_f, is the net energy output of the entire PV system (AC) per rated kilowatt (DC) of the installed PV array:

$$Y_f = E_{out} / P_0 \tag{6}$$

The reference yield (Y_r) of a monofacial PV system is calculated by dividing the total front-side in-plane irradiance by the module's reference plane-of-array irradiance:

$$Y_r = H_i / G_{i,ref} \tag{7}$$

Where the reference plane-of-array irradiance, represented as $G_{i,ref}$ [kW·m^{-2}] is the irradiance at which P_0 is determined, typically specified under standard test conditions.

As well as the total system irradiation, it should be noted that there are PV arrays corresponding to each subsystem or PV roof with different tilt and orientation, so that a weighted reference yield $Y_{r,weighted}$ should be calculated:

$$Y_{r,weighted} = H_{i,weighted} / G_{i,ref} \tag{8}$$

The yield losses are determined by subtracting yields. They are expressed in [kWh· kW^{-1}] (or h) and represent the amount of time the array would have to operate at its rated power (P_0) to compensate for the corresponding losses observed during the reporting period.

The array capture loss, referred as L_c, represents the losses attributed to operational factors of the array, such as losses in wiring and junction boxes prior to DC measurement, array temperature effects, soiling, etc. It is formally defined as:

$$L_c = Y_r - Y_A \tag{9}$$

The balance of system (BOS) loss, referred to as L_{BOS}, quantifies the losses in the BOS components, including the inverter, as well as all wiring and junction boxes that are not taken into account in array capture loss. It is defined as:

$$L_{BOS} = Y_A - Y_f \tag{10}$$

The rated array efficiency is given by:

$$\eta_{A,0} = P_0 / (G_{i,ref} \times A_a) \tag{11}$$

In this context, the total area of the array (A_a) is calculated as the sum of the front areas of the PV modules as defined by their outer edges.

The mean system efficiency over the reporting period is defined by:

$$\eta_f = E_{out} / (H_i \times A_a) \tag{12}$$

The parameter η_{BOS}, which represents the BOS efficiency over the reporting period, is defined as:

$$\eta_{BOS} = E_{out} / E_A \tag{13}$$

The performance ratio is defined as the ratio of the Y_f to its Y_r. It serves to quantify the overall impact of production losses within the system, arising from factors such as array temperature, inefficiencies and failures in system components. It includes considerations on the balance of the system components:

$$PR = Y_f / Y_r \tag{14}$$

The capacity utilisation factor is a metric that is estimated in power plants and allows comparison between different plants. Its calculation is based on the rated AC power ($P_{0,AC}$) of the system and defines the fraction of electrical energy generated compared to the energy that would have been generated by operating at 100 % of its rated AC power during the reporting period, typically 365 days.

$$CUF = \left(\frac{E_{out}}{P_{o,CA}} \right) \Big/ (24h \times days) \tag{15}$$

The performance metrics defined in the standard are not mandatory across all types of plants, and their application may vary depending on the system design and the specific requirements of the user. Furthermore, the selection of certain metrics over others can significantly impact their usefulness, depending on the context and the particular application for which they are employed.

To conduct a more detailed assessment of the performance of self-consumption PV systems and considering the specific characteristics of these systems, additional innovative parameters can be calculated to provide further insight into performance analysis, as suggested by Muñoz-Rodríguez et al (Muñoz-Rodríguez et al., 2023). These parameters are based on the calculation of self-consumption productivity indices and non-self-consumed energy indices. Similar to those proposed by the standard, they are defined per kW, allowing for comparisons between PV self-consumption systems of different capacities.

To estimate these parameters, it is necessary to determine the self-consumed PV power (P_{PVSC}). This parameter can be estimated as the minimum value between the inverter output power, P_{out}, and the power demanded by the load, P_L. In this context, the self-consumed PV power (P_{PVSC}) corresponds to P_L.

$$P_{PVSC} = \min[P_{out}, P_L] \tag{16}$$

Self-consumed PV energy (E_{PVSC}) can be estimated by calculating the area under the P_{PVSC} profile. This represents the energy directly consumed by the loads within a given reporting period.

$$E_{PVSC} = \sum_k P_{PVSC,k} \times \tau_k \tag{17}$$

Thus, the final self-consumption yield can be defined, indicating the self-consumed energy per kW as:

$$Y_{f,PVSC} = \frac{E_{PVSC}}{P_0} \tag{18}$$

This parameter can be useful for comparing self-consumption PV systems with different array capacities. If no storage system is considered, the energy that is not directly self-consumed can be exported to the grid (E_{TG}). Thus, the final to grid yield can be used, as described in the following equation:

$$Y_{f,TG} = \frac{E_{TG}}{P_0} = Y_f - Y_{f,PVSC} \tag{19}$$

These productivity indices not only provide information on the level of self-consumption but also offer insights into the proper operation of the PV array. To analyse the interaction of grid energy with the total load consumption, the load ratio (GL) can be used (Gergely et al., 2022; Jimenez-Castillo et al., 2023). This parameter describes the amount of energy transferred at a given node in the grid without considering the direction of the flow:

$$GL = \frac{E_{TG} + E_{FG}}{E_L} = \frac{E_{GL}}{E_L} \tag{20}$$

Where E_{FG} corresponds to the energy imported from the electricity grid and E_{GL} to the energy transferred to utility grid at the given node.

Zero indicates that there is no energy interaction with the grid. In cases where there is no PV generator or it is not operational, this ratio may be one. Additionally, it can be one when the energy exported to the grid equals the energy consumed by the load, so the PV system generates just twice as much as the load consumes ($E_{TG} = E_L$ & $E_{FG} = 0$). If the load consumption is equal to the energy interaction occurring at the grid connection node, this index can also obtain the value one. Finally, this index has a minimum value at which there is less energy exchange with the grid. This point presents an inflection and trend change of this index.

Following this index, different performances yields are proposed which are referred to the nominal or design connection capacity between the system and the grid (P_{des}).

$$Y_{GL} = \frac{E_{GL}}{P_{des}} = \frac{E_{TG} + E_{FG}}{P_{des}} = \frac{E_{TG}}{P_{des}} + \frac{E_{FG}}{P_{des}} = Y_{GL,TG} + Y_{GL,FG} \tag{21}$$

Y_{GL} represents the hours of operation that the connection node is operating at maximum capacity. $Y_{GL,TG}$ and $Y_{GL,FG}$ represent the equivalent hours when the grid is operating at full capacity, depending on the direction of flow.

A complementary performance indicator is proposed to quantify the duration during which the industrial facility consumes power at or above the contracted grid capacity. This metric, referred to as the Equivalent Capacity Utilisation Yield (Y_L), is defined as the total number of hours within the analysis period during which the instantaneous power demand equals the contracted power level or the capacity of the grid connection node.

$$Y_L = \frac{E_L}{P_{des}} \tag{22}$$

The Y_L expresses the number of equivalent full-load hours at contracted power that correspond to the facility's actual energy consumption. It serves as a normalised metric to evaluate the extent to which the contracted connection capacity is used. Higher Y_L values indicate efficient use of the available capacity, while lower values may point to overdimensioning or low operational demand.

The performance evaluation of rooftop self-consumption PV systems in industrial environments requires analysis tools that go beyond the traditional indicators proposed by standards such as IEC 61724. In this context, the introduction of innovative metrics such as $Y_{f,PVSC}$, $Y_{f,TG}$, Y_{GL}, and Y_L could provide a more accurate and detailed view of the operational behaviour of self-consumption systems. These metrics make it possible to quantify energy production and understand energy exchange dynamics, self-consumption levels, sizing efficiency and grid connection stability.

$Y_{f,PVSC}$ and $Y_{f,TG}$ provide a differentiation between self-consumed energy and energy fed into the grid. These indices make it possible to measure the amount of energy generated and to assess the degree of energy self-sufficiency achieved by the system. Likewise, Y_{GL} makes it possible to quantify the energy transferred without taking into account the direction of the flow, providing clues about the use of grid connection node. Finally, Y_L facilitates the evaluation of the increase or decrease in the use of the electrical grid connection node after the incorporation of PV systems.

These metrics complement and enrich the traditional analysis of the standard, offering a more holistic perspective adapted to the specific challenges posed by industrial rooftop PV self-consumption systems but aligned with the standard methodology, allowing direct comparison of different systems and loads.

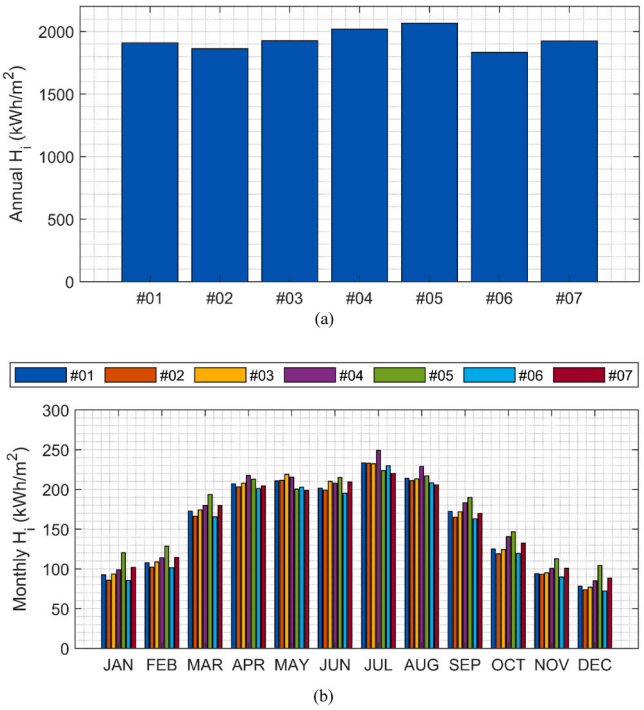

Fig. 5. Annual (a) and monthly (b) in-plane irradiation corresponding to the seven PV systems.

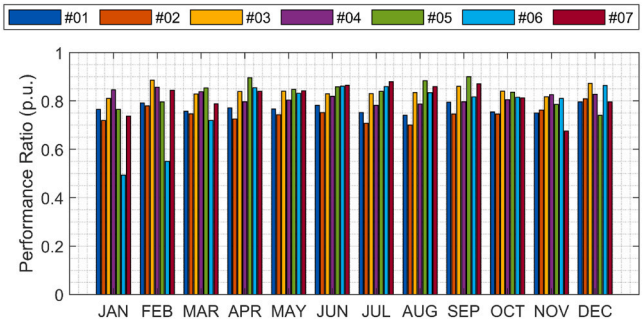

Fig. 6. Performance Ratio (PR) calculated for each system.

Results

This section presents the results from the seven analysed PV systems. First, the performance parameters of the PV systems are described, followed by those related to the interaction between the PV system and the

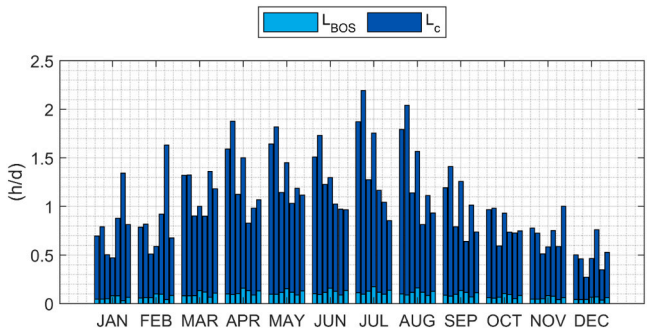

Fig. 7. Monthly average capture and balance of system losses for each system.

industrial loads, as well as the parameters associated with the grid interaction.

Performance Metrics of Rooftop PV Systems

The seven previously described PV systems have been analysed under real operating conditions over a one-year period. Fig. 5 presents the monthly and annual in-plane irradiation recorded in the different PV systems. For systems with different orientations, the weighted in-plane irradiation (Eq. 8) is presented, which will be used to evaluate the overall system performance.

The upper chart (a) displays the annual irradiation values for each system, showing variations among them (<12 %). It is observed that the values of annual H_i range from 1833.87 kWh/m^2 for system #06 to 2064.78 kWh/m^2 for system #05, reflecting differences in solar resource availability at each location. This represents a variation of 11.2 %. In general, the values of Hi are aligned with the average solar irradiation at the systems sites (Andalusia, ~1800–1900 kWh/m^2 per year) (Ordóñez et al., 2010). On the other hand, the lower chart (b) represents the monthly in-plane irradiation distribution. The data show seasonal variations, with the highest irradiation levels occurring between April and August, and the lowest values observed from November to February. Systems #04 and #05 show higher irradiation during the summer and winter months, compared to the other systems.

Fig. 6 presents the evolution of the monthly PR for the seven systems. The calculated and displayed monthly PR is determined based on the monthly Y_f and Y_r of each system.

The highest PR values are recorded in February for systems #03 (0.87) and #04, while for systems #01, #02, and #06 (0.86), the highest values are observed in December. On the other hand, system #05 (0.90) shows its peak value in September, and system #07 in July. Regarding the minimum values, these are recorded in August for systems #01 and #02, and in July for systems #04. In contrast, system #07 shows its minimum in November, while systems #03 and #06 reach their minimums in January, months characterised by colder climatic conditions. Regarding system #06, the very low values of PR are due to the different inverter configuration, as previously mentioned.

Fig. 7 shows the monthly results of losses in the BOS and capture losses. The L_{BOS} losses exhibit relatively low values throughout all the months analysed. In contrast, the L_c losses show greater temporal variability. For example, in system #06, the highest L_c values are recorded in January and February, while in the rest of the systems, the largest losses are concentrated in the spring and summer months.

The results of the annual parameters and metrics for the systems are shown in Table 5. The columns correspond to each of the analysed systems. The different orientations (S, E-W, S-E-W) are also presented.

The Y_r values for the studied systems are relatively similar, with a relative difference between the highest (system #05) and the lowest (system #06) of 11.2 %, both having an E-W orientation. Y_f follows a similar trend to Y_r, with system #05 having the highest value and, in this case, system #02 having the lowest, with a difference of 18.8 %. Y_f values range from 4.48 h/d to 3.76 h/d, values that, as seen in Table 3, are within the reported values for both the module technology and inverters used in different plants.

The L_c losses are higher in system #02 (464.28 kWh/kW), nearly doubling those in system #03 (259.60 kWh/kW). Regarding L_{BOS}, which are associated with electrical components and interconnection, they are higher in system #04 (45.99 kWh/kW) and lower in system #06 (24.01 kWh/kW), just over half. On the other hand, consistency is observed in $\eta_{A,0}$ around 0.20 – 0.21 p.u. The final efficiency (η_f) shows more

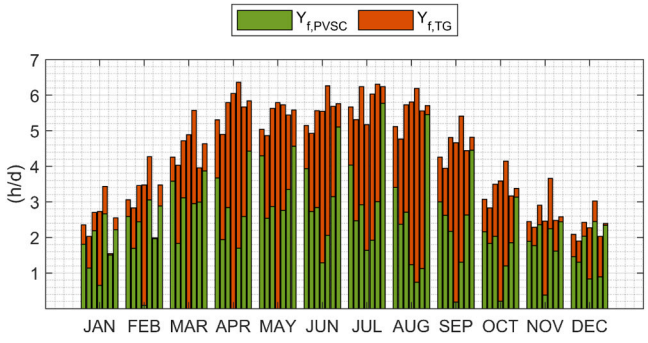

Fig. 8. Monthly average Final self-consumption and Final to grid yield for each system.

Table 5
Annual results of performance parameters for each system.

Parameter	#01	#02	#03	#04	#05	#06	#07
P_0 (kW)	54.39	44.10	37.24	3.64	16.20	50.40	18.00
Orientations	S – E - W	E - W	S	S	E - W	E - W	S
H_i (kWh/m^2)	1908.31	1862.02	1926.52	2020.03	2064.78	1833.87	1924.81
E_A (kWh)	81,205.01	61,640.31	62,076.06	6096.86	27,960.04	75,306.12	29,770.63
E_{out}(kWh)	79,649.56	60,458.07	60,909.71	5929.46	27,382.67	74,105.60	29,092.77
Y_A kWh· kW^{-1} (or h)	1493.01	1397.74	1666.92	1674.96	1725.93	1506.12	1653.92
Y_f kWh· kW^{-1} (or h)	1464.42	1370.93	1635.59	1628.97	1690.29	1482.11	1616.27
Y_r kWh· kW^{-1} (or h)	1908.31	1862.02	1926.52	2020.03	2064.78	1833.87	1924.81
L_c kWh· kW^{-1} (or h)	415.29	464.28	259.60	345.08	338.86	327.75	270.88
L_{BOS} kWh· kW^{-1} (or h)	28.59	26.81	31.32	45.99	35.64	24.01	37.66
$\eta_{A,0}$ (p.u)	0.21	0.21	0.21	0.21	0.20	0.20	0.20
η_f (p.u)	0.16	0.15	0.18	0.17	0.17	0.16	0.18
η_{BOS} (p.u)	0.98	0.98	0.98	0.97	0.98	0.98	0.98
PR (p.u)	0.77	0.74	0.85	0.81	0.82	0.81	0.84

Table 6
Annual results of load and grid interaction parameters for each system.

Parameter	#01	#02	#03	#04	#05	#06	#07
Orientations	S – E - W	E - W	S	S	E - W	E - W	S
P_{des} (kW)	95.00	47.60	35.00	6.93	20.00	99.00	18.00
$Y_{f,PVSC}$ kWh· kW^{-1} (or h)	1090.43	737.53	928.78	199.26	657.28	811.39	1421.00
$Y_{f,TG}$ kWh· kW^{-1} (or h)	373.99	633.40	706.81	1429.71	1033.01	670.72	195.27
Y_L kWh· kW^{-1} (or h)	2277.79	1580.29	1584.98	938.79	1665.93	1423.93	4368.98
Y_{GL} kWh· kW^{-1} (or h)	1862.59	1472.30	1340.90	1578.15	1931.41	1347.12	3139.64
$Y_{GL,TG}$ kWh· kW^{-1} (or h)	209.10	575.31	744.13	734.09	819,76	336.27	191.66
$Y_{GL,FG}$ kWh· kW^{-1} (or h)	1653.49	896.99	596.77	844.07	1111.65	1010.86	2947.98
CUF (p.u)	0.18	0.17	0.19	0.23	0.21	0.14	0.22

significant variation between systems, being highest in system #03 (0.18 p.u) and lowest in system #02 (0.15 p.u). η_{BOS} also shows minor variability, with slightly higher values in system #06 (0.98 p.u.) and lower values in system #04 (0.97 p.u.).

System #03 has the highest annual PR (0.85 p.u), while system #02 has the lowest PR (0.74 p.u). As previously mentioned, the PR value may, in some cases, not reflect a high value, even when the system operates according to the operational requirements.

Interaction between solar generation, industrial load and the electrical grid

To extend the performance evaluation of PV self-consumption systems on industrial rooftops, the calculation of the innovative metrics that provide relevant information about the system's interaction with the electrical grid and the load was carried out. Fig. 8 shows the monthly results of the final self-consumption yield and final to grid yield.

The typical seasonal pattern of the location of the PV systems is observed, similar to that shown in Fig. 5, with higher energy generation during the spring and summer months (from April to August), coinciding with the periods of higher irradiance and sunlight hours. Differences in performance metrics ($Y_{f,PVSC}$ and $Y_{f,TG}$) are observed between the different systems. Notably, the reduced $Y_{f,PVSC}$ of system #04, especially from February to May, stands out. This is due to the lack of production activity in the industry during these months, although the PV system continued to operate, exporting all the PV generation to the grid. System #07 presents consistently low $Y_{f,TG}$ values throughout all months, as the entire electrical energy generated by the PV system is consumed directly by the internal loads of the industry. In the case of system #06, as previously mentioned, it is observed that $Y_{f,TG}$ is zero during the months of January and February.

The results of the annual parameters and metrics related to the interaction with the load and the electrical grid of the systems are shown in Table 6. The columns correspond to each of the analysed systems.

$Y_{f,PVSC}$ was highest in system #07, with 1421.00 kWh·kW^{-1} , and lowest in system #04, with 199.26 kWh·kW^{-1} , whereas $Y_{f,TG}$ showed the opposite trend. The values for system #02 are notable, where it self-consumes just over half of what it exports. The CUF reached its maximum value in system #04, with 0.23 p.u., while the minimum was recorded in system #06, with 0.14 p.u, indicating a lower utilisation of its nominal installed peak power throughout the year.

Regarding Y_L, the maximum was observed in system #07, with 4368.98 kWh·kW^{-1} , and the minimum in system #04, with 938.79 kWh·kW^{-1} . This implies that system #07 has a more demanding load and intensive industrial usage. Intermediate values are observed in systems #01 and #05 (2277.79 and 1665.93 kWh·kW^{-1}, respectively), which point to more moderate industrial activity. As for Y_{GL}, its maximum value is recorded in system #07 with 3139.64 kWh·kW^{-1} , while the minimum is observed in system #03 with 1340.90 kWh·kW^{-1} . Notably, systems #01 and #05 also show high values, reflecting a higher degree of utilisation of the grid.

Disaggregating these losses by flow direction provides further clarity. The value $Y_{GL,TG}$ is most pronounced in system #03 (744.13 kWh·kW^{-1}) and system #02 (575.31 kWh·kW^{-1}). These values point to a higher dependency or interaction with imported electricity. Conversely, system #07 displays the lowest $Y_{GL,TG}$ (191.66 kWh·kW^{-1}), indicating minimal grid-to-system input, which could be attributed to high self-sufficiency. In contrast, system #07 once again stands out with a dominant value of $Y_{GL,FG}$ (2947.98 kWh·kW^{-1}), highlighting intensive energy injection into the grid. This is in sharp contrast to system #03, which reports the lowest value (596.77 kWh·kW^{-1}), indicative of reduced surplus generation or limited grid export capacity. Systems #01, #05, and #06 also show considerable $Y_{GL,FG}$ values (1653.49, 1111.65, and 1010.86 kWh·kW^{-1}, respectively), suggesting relatively high levels of exported energy (Ocampo et al., 2021).

Discussion

This section presents a brief discussion related to the operating parameters of the PV systems, followed by the indicators related to the interaction between the PV system and the industrial loads, as well as the parameters associated with the grid interaction.

Performance parameters

The analysis of performance parameters reveals that the highest PR values were recorded in February for systems #03 and #04, whereas for systems #01, #02, and #06, the maximum PR values were observed in December. This finding suggests that, in five out of the seven systems analysed, the periods of highest PR coincide with the winter months. Such behaviour is consistent with previous studies conducted on PV systems installed on building rooftops at the University of Jaén campus (Muñoz-Rodríguez et al., 2025).

System #02 showed the lowest PR, a result that is directly linked to its reduced Y_f (the lowest among all systems) and the highest L_c. Consequently, the diminished PR can be primarily attributed to systematic shading effects. In the specific case of system #06, the notably low PR values can be primarily attributed to its distinctive inverter configuration, as previously discussed. Between January and March, the inverter was programmed to limit energy injection into the public grid at the connection node with the industrial facility. Since the nominal capacity of the PV generator considerably exceeds the electrical demand of the installation, the inverter predominantly operated outside the MPP.

This operational condition results in increased energy capture losses and, consequently, a significant reduction in the system's overall efficiency. Nonetheless, it is important to emphasise that, despite the decrease in PR, the PV generator continued to operate within the specific technical and operational requirements defined by the user and the connection conditions. Similar scenarios have been documented in the literature, where monthly PR values as low as 0.38 have been reported under comparable operational constraints (Jiménez-Castillo et al., 2024).

The observed disparities in PR among the different systems can be explained by several interconnected factors. Predominantly, variations in weather conditions, such as ambient temperature fluctuations and soiling, play a crucial role. Moreover, seasonal changes further contribute to the variability in system performance (Ogliari et al., 2023).

Regarding Y_f, a trend similar to that of Y_r is observed. System #05 registers the highest Y_f values, whereas system #02 exhibits the lowest, with a notable difference of 18.8 %. This considerable disparity is likely associated with shading issues, given that system #02 also demonstrates the highest energy capture losses among the systems analysed.

Load and grid interaction parameters

The study of load and grid interaction parameters reports significant variations among the systems evaluated. Overall, $Y_{f,PVSC}$ reaches higher values in some systems, such as systems #01 and #07. In system #02, it is noteworthy that the amount of energy self-consumed slightly exceeds half of the energy exported. These differences highlight the influence of system-specific characteristics, such as load profiles, system sizing, operational strategies, and the extent to which generation matches instantaneous consumption demands. In contrast, other systems (#04 and #05), display significantly higher $Y_{f,TG}$ values, indicating that a substantial portion of the generated energy is fed into the grid. This may be the result of intermittent or limited on-site load, oversized generation capacity, or a lack of demand-response integration. In particular, systems with very low self-consumption appear to operate under conditions where local energy demand does not effectively match with the PV generation, leading to increased export to the grid. Such configurations might benefit from the implementation of storage solutions or demand-shifting strategies to enhance self-consumption and reduce grid dependency.

Assessing the metrics, it becomes evident that the temporal resolution of the analysis, monthly versus annual, has a significant impact on the interpretation of system performance. Annual values provide a general overview of the energy balance between self-consumption and grid export, offering a summary of the system's long-term efficiency and overall energy management. However, this aggregated perspective may conceal short-term operational behaviours, such as periods of inactivity, seasonal mismatches between generation and demand, or temporary shifts in consumption patterns.

Monthly analysis allows for the identification of critical operational anomalies or trends that are otherwise obscured in annual summaries. For instance, in the case of system #04, the monthly data reveals that during February, March, April and May, there is an absence of local consumption, resulting in the full export of generated energy to the grid. This behaviour is not readily apparent from annual data, when compared with the results obtained from the other systems. Detecting these deviations is essential for diagnosing operational issues.

With regard to Y_L, Y_{GL}, $Y_{GL,TG}$ and $Y_{GL,FG}$, these metrics enable the quantification of the number of equivalent full-load hours during which the interconnection node between the industrial facility and the power grid operates at its nominal capacity. In systems #01, #02, #03, #06 and #07, a reduction in these equivalent hours is observed following the integration of rooftop PV systems, as the values of Y_{GL} are consistently lower than those of Y_L. This reduction is particularly notable in system #07, with a reduction of 28.1 %. Such a decrease indicates reduced utilisation of the contracted grid capacity as a result of the contribution from locally generated PV energy. The metrics Y_{GL} and Y_L are useful for assessing the degree of utilisation of the grid connection node before and after the integration of the PV system, expressed in terms of equivalent full-load operating hours. Their comparison facilitates the analysis of whether the PV system leads to a reduction or increase in the facility's energy dependence on the power grid.

In all the industrial sites analysed, the equivalent operation of the interconnection node from the facility to the grid, represented by the indicator $Y_{GL,TG}$, is significantly reduced with the incorporation of PV systems. This reduction ranges from 37 % in industry #01–89 % in industry #04, highlighting a substantial decrease in dependence on the conventional electrical grid.

Furthermore, the highest values of the metric $Y_{GL,TG}$, observed in industries #03, #04 and #05, indicate a greater use of the connection node for the export of surplus PV energy to the grid. This may be attributable to a lower matching between generation and consumption, a relative oversizing of the PV system, or an operational strategy aimed at maximising energy production.

In contrast, industries such as #01, #06 and #07 exhibit higher values of $Y_{GL,FG}$, indicating that the connection node continues to be used primarily for importing energy from the grid. This behaviour may be linked to insufficient PV generation capacity to meet demand, low temporal matching between solar production and consumption, or high energy consumption during periods without generation (e.g., night shifts or weekends with low irradiance). In these cases, the self-consumption system partially reduces dependence on the grid, but does not significantly displace the use of the connection node for conventional energy supply.

The interaction between PV systems, the load, and the electrical grid is a critical factor influencing the reliability and stability of the energy supply. The analysis of these parameters enables a better understanding of the efficiency that PV systems are integrated into existing grids and the demand on them. Optimising such integration is fundamental to minimising losses and mitigating voltage deviations, thereby improving voltage profiles and overall network performance, particularly under variable load and solar resource conditions (Bahari et al., 2023).

The CUF ranged between 0.14 p.u. in system #06 and 0.23 p.u. in system #04. These values are consistent with those typically reported for PV systems operating under self-consumption schemes, where CUF values below 0.25 p.u. are common. The value of CUF for such plants is in range of 0.10–0.25 (Kumar et al., 2020). Such behaviour is primarily due to the inherent daily and seasonal variability of solar irradiance and the frequent absence of energy storage solutions. Differences in CUF among systems can be attributed to several factors, including module orientation, local irradiance conditions, the match between generation and instantaneous consumption, as well as possible design or operational limitations. Although the CUF provides a first approximation of each system's energy utilisation level, its interpretation must be complemented with other performance metrics. This is particularly relevant in self-consumption installations, where maximising energy generation is not necessarily the main objective, but rather adapting to the specific demand profiles of the facility. An example is the configuration of the

inverter to avoid feeding energy into the grid. The PV system may appear to be malfunctioning; however, this is a customer or load requirement.

Conclusions

The results of the analysis of 106 studies indicate that PR is the most commonly used parameter in the performance evaluation of PV systems, present in 97.17 % of the studies, followed by Y_f at 83.96 % and CUF at 65.09 %. For the most commonly used metrics (PR and Y_f), no significant correlation is observed based on the peak power capacity, which aligns with previous studies that discard a relationship between PR and latitude or system power. The annual PR values of the study vary between 0.74 and 0.85 p.u., showing the diversity of yields influenced by the properties of each system and the actual operating conditions in a continental Mediterranean climate.

Additionally, no significant differences in PR and Y_f values are identified across the three module technologies analysed, which could be attributed to factors such as degradation, climatic variability, and maintenance management. Therefore, it is recommended that future studies expand the availability of operational and environmental data and delve deeper into the analysis of all elements, considering additional factors to gain a more comprehensive understanding of the behaviour of the PV systems under study. One of them may be the commissioned date of the systems.

Regarding inverter technology, the central inverter configuration is the most reported, followed by the multi-MPPT configuration, which shows higher PR and Y_f values. The multi-MPPT configuration is preferred in small and medium-scale systems due to its modularity, reliability, and energy efficiency. In this context, multi-MPPT inverters can enhance the integration of renewable energies and serve as a viable option for rooftop PV systems.

Finally, this study presents the operational analysis of seven rooftop PV systems installed on industrial buildings under real operating conditions, through the calculation of various indices proposed by standards that can be highly useful. These include performance metrics, performance coefficients, efficiencies, and losses, as well as the new proposed yields Y_L, Y_{GL}, $Y_{GL,TG}$ and $Y_{GL,FG}$, among other indices evaluating the system's interaction with the grid proposed by the scientific community.

The results from one year of monitoring demonstrate that these indices are suitable for analysing the performance of PV systems with direct self-consumption, as well as providing insights into how these systems interact with the industrial loads and the electrical grid. Although most systems operate close to expectations, with PR, Y_f and CUF annual averages of 0.81, 1555.51 h/y and 0.19 respectively, factors such as partial shading, capture losses, and inverter configurations without grid injection affect their efficiency. Regarding new proposed yields, in systems #01, #02, #03, #06 and #07, a reduction in the full-load equivalent hours during which the interconnection node between the industrial facility and the power grid operates at its nominal capacity is observed following the integration of rooftop PV systems, as the values of Y_{GL} are consistently lower than those of Y_L. This reduction is particularly notable in system #07, with a reduction of 28.1 %.

The use of indices proposed in the literature can complement the information provided by existing standards metrics. These indices address the interaction with the grid at the system level, considering both the use and generation of energy on-site. Regarding data availability and suitability, a monthly resolution seems to be an appropriate level for characterising the main differences between systems performance and their configurations. Monthly data takes into account seasonal effects, which reflect the mismatch between load and generation. It was identified that the differences between the actual and the expected behaviour of the systems are significant, mainly influenced by their design, location, and operating conditions.

CRediT authorship contribution statement

J.L. Sánchez-Jiménez: Writing – review & editing, Writing – original draft, Investigation, Data curation, Formal analysis. **G. Jiménez-Castillo:** Supervision, Writing – review & editing, Writing – original draft, Project administration, Investigation, Conceptualization, Formal analysis. **C. Rus-Casas:** Supervision, Project administration, Investigation, Formal analysis, Writing – review & editing. **A.J. Martínez-Calahorro:** Project administration, Investigation, Writing – review & editing. **F.J. Muñoz-Rodríguez:** Supervision, Project administration, Investigation, Formal analysis, Writing – review & editing.

Declaration of Generative AI and AI-assisted technologies in the writing process

During the preparation of this work the author(s) used ChatGPT and Gemini in order to translate and improve the readability and language of the manuscript. After using this tool/service, the author(s) reviewed and edited the content as needed and take(s) full responsibility for the content.

Declaration of Competing Interest

The authors declare that they have no known competing financial interests or personal relationships that could have appeared to influence the work reported in this paper.

Acknowledgement

The work was supported by the projects oriented towards the ecological transition and the digital transition. (Grant No. TED2021–131137B-I00 ("Aportación a la Transición Ecológica en el sector Industrial a través del Autoconsumo Fotovoltaico") and "Centro para el Desarrollo Tecnológico Industrial (CDTI)" and "Corporación Tecnológica de Andalucía (CTA)" under the project: "SolAGRO+ . Análisis funcional avanzado predictivo para la mejora de la gestión del mantenimiento de sistemas de autoconsumo solar fotovoltaico en sector de la industria agroalimentaria. The authors also acknowledge the support provided by the Thematic Network 723RT0150 "Red para la integración a gran escala de energías renovables en sistemas electricos (RIBIERSE-CYTED)" financed by the call for Thematic Networks of the CYTED (Ibero American Program of Science and Technology for Development) for 2022. The authors would like to thank the University of Jaén for its support by the programme: "Acción 2. Doctorados en entidades externas comprendida en la "Línea de Actuación: Fomento y divulgación de la transferencia", enmarcada en el Objetivo 1: "Apoyo a las actividades de trasferencia del conocimiento", del Plan de Apoyo a la Transferencia del Conocimiento, el Emprendimiento y la Empleabilidad año 2023, para la contratación de doctorandos industriales".

Appendix A

Table A
Primary performance analysis parameters derived from the monitored data that have been used in the literature

Ref.	Year	Loc.	Configuration	Peak power (P0)	Reference yield (Yr)	Array yield (Y_A)	Final yield (Y_f)	Performance Ratio (PR)	Performance Ratio corrected by temperature (PRT)	Capacity utilization factor (CUF)	PV array efficiency (n_a)	Inverter efficiency (n_{inv})	System efficiency (n_{sys})	Balance of system efficiency (n_{BOS})	Array capture loss (L_c)	Balance of system Loss (L_{BOS})	Cell Temperature Loss (L_T)	Total loss (Lt)
(Iftikhar et al., 2021)	2021	Pakistan	On-Grid. Ground Utility scale	18 MW				x										
(Bansal et al., 2022a)	2022	India	On-Grid. Ground Utility scale	10 MW	x	x	x	x		x	x		x		x	x		
(Heyine et al., 2022)	2022	Mauritania	On-Grid. Utility scale	50 MW	x	x	x	x			x		x		x	x		
(Berastain et al., 2022)	2022	Perú	On-Grid. Rooftop	3x1.5 kW	x		x	x										
(Maurya et al., 2022)	2022	India	On-Grid. Rooftop	40 kW	x	x	x	x			x		x		x	x		x
(K et al., 2018)	2018	India	On-Grid. Rooftop	40 kW	x	x	x	x		x	x		x	x	x	x		
(Haffaf et al., 2021)	2021	France	On-Grid. Rooftop	2.4 kW			x			x								
(El Hacen Jed et al., 2020)	2020	Mauritania	On-Grid. Ground Utility scale	950 kW	x	x	x	x		x	x		x	x	x	x		
(Bouacha et al., 2020)	2020	Algeria	On-Grid. Rooftop	9.5 kW	x	x	x	x			x		x	x	x	x		
(Sharma and Goel, 2017)	2017	India	On-Grid. Rooftop	11.2 kW	x	x	x	x		x	x		x	x	x	x		
(Yadav and Bajpai, 2018)	2018	India	On-Grid. Rooftop	5 kW	x	x	x	x		x	x		x	x	x	x		
(Attari et al., 2016)	2016	Morocco	On-Grid. Rooftop	5 kW	x	x	x	x		x	x		x	x	x	x		
(Thotakura et al., 2020)	2020	India	On-Grid. Rooftop Utility Scale	1 MW			x	x		x								
(Okello et al., 2015)	2015	Africa	On-Grid. Rooftop	3.2 kW	x		x	x		x						x		
(Al-Otaibi et al., 2015)	2015	Kuwait	On-Grid. Rooftop	106.6 kW		x	x	x										
(Dabou et al., 2016)	2016	India	On-Grid. Ground	1.75 kW	x	x	x	x			x		x	x	x	x		
(Narasimman et al., 2023)	2023	India	On-Grid. Ground Utility scale	5 MW				x		x								
(Mpholo et al., 2015)	2015	Lesotho	On-Grid. Ground	281 kW	x	x	x	x		x	x		x	x	x	x		
(Daher et al., 2018)	2018	Yibuti	On-Grid. Ground	302.4 kW	x	x	x	x		x	x		x	x	x	x		
(Mohammed et al., 2022)	2022	Saudi Arabia	On-Grid. Rooftop	10 kW			x	x										
(Shuvho et al., 2019)	2019	Bangladesh	On-Grid. Rooftop	80 kW		x	x	x										
(Santiago et al., 2018)	2018	Spain	On-Grid. Rooftop	100 kW	x	x					x				x			
(Chandel and Chandel, 2022)	2022	India	On-Grid. Ground Utility scale	19 MW	x	x	x	x		x					x	x		
(Bentouba et al., 2021)	2021	Algeria	On-Grid. Ground Utility scale	20 MW	x		x	x		x								
(Akhter et al., 2020)	2020	Malaysia	On-Grid. Rooftop	6.575 kW	x	x	x	x			x		x	x	x	x		
(Oloya et al., 2021)	2021	Uganda	On-Grid. Ground Utility scale	10 MW			x	x		x								
(Minai et al., 2022)	2022	India	On-Grid. Rooftop	467.2 kW				x		x								

(*continued on next page*)

Table A (*continued*)

(Shiva Kumar and Sudhakar, 2015)	2021	India	On-Grid. Rooftop	100 kW		x	x	x		x			x	x	x	x		
(Dobaria et al., 2016)	2016	India	On-Grid. Rooftop	5.05 kW	x	x	x	x							x	x		
(Mukherji et al., 2020)	2019	India	On-Grid. Rooftop	50 kW	x		x	x		x								
(Al-Aboosi and Al-Aboosi, 2021)	2021	USA	On-Grid. Rooftop	3.36 MW	x	x	x	x		x								
(Bansal et al., 2022b)	2022	India	On-Grid. Ground Utility scale	9 MW	x	x	x	x		x			x		x	x	x	
(Veerendra Kumar et al., 2022)	2022	USA	On-Grid. Ground Utility scale	1.1 MW	x		x	x		x			x					
(Santiago et al., 2017)	2017	Spain	On-Grid. Rooftop	17.8 kW	x	x	x	x	x		x		x	x	x	x		
(Sidrach-De-Cardona and López, 1998)	1998	Spain	On-Grid. Rooftop	2 kW			x	x										
(Fuster-Palop et al., 2022)	2022	Spain	On-Grid. Ground Utility scale	50 MW	x		x	x		x	x		x	x	x	x		
(Martín-Martínez et al., 2019)	2019	Spain	On-Grid. Ground Utility scale	2.7 MW 1.4 MW 370 kW 1.3 MW 1.3 MW 4.6 MW	x		x	x		x			x					
(Ayora et al., 2023)	2023	Kenya	On-Grid. Rooftop	600 kW	x	x	x	x		x					x	x		x
(Muñoz-Rodríguez et al., 2023)	2023	Spain	On-Grid. Rooftop	2.97 kW	x	x	x	x						x	x	x		
(Montes et al., 2022)	2022	Spain	On-Grid. Ground Utility scale	13 MW				x										
(Abdullah and Nishimura, 2021)	2021	Japan	On-Grid. Rooftop	40.1 kW	x	x	x	x		x					x	x		
(Roy et al., 2021)	2021	United Arab Emirates	On-Grid. Ground Utility scale	18 MW				x		x			x					
(Castrillón-Mendoza et al., 2020)	2020	Colombia	On-Grid. Rooftop	152 + 248 kW	x		x	x										
(Jed et al., 2021)	2021	France	On-Grid. Ground Utility scale	4.5 MW	x		x	x	x									
(Boddapati et al., 2021)	2019	India	On-Grid. Ground Utility scale	50 MW				x		x								
(Dahmoun et al., 2021)	2017–2020	Algeria	On-Grid. Ground Utility scale	23.92 MW		x	x	x		x								
(Sreenath et al., 2020)	2020	Malaysia	On-Grid. Ground Utility scale	20 MW	x	x	x	x		x			x		x	x		
(Elhadj Sidi et al., 2016)	2015	Mauritania	On-Grid. Ground Utility scale	15 MW		x	x	x		x					x	x		
(Sukumaran and Sudhakar, 2017)	2016	India	On-Grid. Ground Utility scale	12 MW	x	x	x	x		x			x					

(*continued on next page*)

Table A (*continued*)

(Shiva Kumar and Sudhakar, 2015)	2015	India	On-Grid. Ground Utility scale	10 MW				x		x								
(Ahmed et al., 2021)		Pakistan	On-Grid. Ground Utility scale	2.5 MW			x	x		x								
(Mensah et al., 2019)	2013–2016	Ghana	On-Grid. Ground Utility scale	2.5 MW				x		x								
(Aslam et al., 2021)	2020	Pakistan	On-Grid. Ground Utility scale	1 MW			x	x		x								
(Malvoni et al., 2017)	2012–2015	Italy	On-Grid. Ground	960 kW	x	x	x	x		x	x		x		x	x		
(Banda et al., 2019)	2013–2017	Malawi	On-Grid. Ground	830 kW	x	x	x	x		x	x		x	x	x	x		
(Chokmaviroj et al., 2006)	2004	Thailand	On-Grid. Ground	500 kW			x	x							x	x		
(Silva et al., 2020)	2019	Brazil	On-Grid. Rooftop	336.96 kW			x	x										
(Satish et al., 2020)	2019	Dubai	On-Grid. Rooftop	200 kW			x	x							x	x		
(Sharma and Chandel, 2013)	2011	India	On-Grid. Ground	190 kW	x		x	x		x			x					
(Kymakis et al., 2009)	2007	Greece	On-Grid. Ground	171.36 kW	x	x	x	x		x					x	x		
(Wittkopf et al., 2012)	2011	Singapore	On-Grid. Rooftop	142.5 kW	x	x	x	x			x		x		x	x		
(Phap and Nga, 2020)	2019	Vietnam	On-Grid. Rooftop	56.7 kW			x	x							x	x		
(Drif et al., 2007)	2003	Spain	On-Grid. Rooftop	40 + 67.84 + 67.84 + 20 kW	x	x	x	x				x	x		x	x		
(Sahouane et al., 2019)	2017–2018	Algeria	On-Grid. Rooftop	28 kW	x	x	x	x		x	x		x	x	x	x	x	
(Al-Badi, 2020)	2014-2018	Oman	On-Grid. Rooftop	20.4 kW	x	x	x	x		x			x		x	x	x	
(Emmanuel et al., 2017)	2014	New Zealand	On-Grid. Rooftop	10 kW	x	x	x	x		x			x	x	x	x		
(Atsu et al., 2021)	2016	Hungary	On-Grid. Rooftop	9.6 kW	x		x	x		x			x		x			
(Mi et al., 2016)	2015	China	On-Grid. Ground	9 kW	x		x	x					x					
(Dondariya et al., 2018)	2018	India	On-Grid. Rooftop	6.4 kW				x										
(Wu et al., 2015)	2009	China	On-Grid. Rooftop	3 kW	x	x	x	x		x	x		x		x	x		
(Piao et al., 2009)	2003	Korea	On-Grid. Rooftop	3 kW	x	x		x			x		x	x	x	x		
(Ameur et al., 2019)	2016	Morocco	On-Grid. Rooftop	2.4 kW			x	x		x			x					
(Haibaoui et al., 2017)	2015	Morocco	On-Grid. Rooftop	5.94 kW				x					x					
(Milosavljević et al., 2015)	2013	Serbia	On-Grid. Rooftop	2 kW	x		x	x		x			x					

(*continued on next page*)

Table A (*continued*)

(Rout and Kulkarni, 2020)	2019	India	On-Grid. Rooftop	2 kW				x										
(Ayompe et al., 2011)	2009	Ireland	On-Grid. Rooftop	1.72 kW	x	x	x	x		x	x		x	x	x	x	x	
(Karna et al., Jan. 2023)	2021-2023	Nepal	Off-Grid. Ground	150 + 75 kW				x		x			x		x	x		
(Emziane and Al Ali, 2015)	-	United Arab Emirates	On-Grid. Rooftop	111.4 + 50.4 + 215.7 + 994 kW			x			x								
(Falih et al., 2022)	-	Iraq	On-Grid. Rooftop	5 kW	x	x	x	x		x	x		x		x	x		
(Mohamed et al., 2024)	2022	Maldives	On-Grid. Rooftop	6.6 kW			x	x		x			x					
(Ateş, 2023)	2018-2020	Turkey	On-Grid. Rooftop	30 kW	x	x	x	x		x					x	x		
(Vidal et al., 2020)	2018	Chile	On-Grid. Ground	8.2 kW			x	x		x					x			
(De Miguel et al., 2002)	2001	Spain	On-Grid. Rooftop	4.3 kW	x	x	x	x			x	x	x		x	x		
(Owolabi et al., 2022)	2021	South Korea	On-Grid. Rooftop	5 + 4.6 kW		x	x	x		x	x	x	x					
(Seme et al., 2019)	2011-2018	Slovenia	On-Grid. Rooftop	111.8 + 5.5 + 47.9 + 12.5 + 7.1 + 58.8 + 71.4 + 4.2 + 77.4 + 335 + 19 + 26.3 + 14.7 + 66.5 kW			x	x		x								
(Piliougine et al., 2013)	2013	Spain	On-Grid. Rooftop	1.17 kW			x	x		x								
(Guerra et al., 2017)	2013-2015	Spain	On-Grid. Rooftop	1.25 + 1.1 kW	x	x	x	x			x	x	x		x	x		
(Yakubu et al., 2024)	2022	Ghana	On-Grid. Ground	50.76 kW	x	x	x	x		x								

(Iftikhar et al., 2021; Bansal et al., 2022a; Heyine et al., 2022; Berastain et al., 2022; Maurya et al., 2022; K et al., 2018; Haffaf et al., 2021; El Hacen Jed et al., 2020; Bouacha et al., 2020; Sharma and Goel, 2017; Yadav and Bajpai, 2018; Attari et al., 2016; Thotakura et al., 2020; Okello et al., 2015; Al-Otaibi et al., 2015; Dabou et al., 2016; Narasimman et al., 2023; Mpholo et al., 2015; Daher et al., 2018; Mohammed et al., 2022; Shuvho et al., 2019; Santiago et al., 2018; Chandel and Chandel, 2022; Bentouba et al., 2021; Akhter et al., 2020; Oloya et al., 2021; Minai et al., 2022; Shiva Kumar and Sudhakar, 2015; Dobaria et al., 2016; Mukherji et al., 2020; Al-Aboosi and Al-Aboosi, 2021; Bansal et al., 2022b; Veerendra Kumar et al., 2022; Santiago et al., 2017; Sidrach-De-Cardona and López, 1998; Fuster-Palop et al., 2022; Martín-Martínez et al., 2019; Ayora et al., 2023; Muñoz-Rodríguez et al., 2023; Montes et al., 2022; Abdullah and Nishimura, 2021; Roy et al., 2021; Castrillón-Mendoza et al., 2020; Jed et al., 2021; Boddapati et al., 2021; Dahmoun et al., 2021; Sreenath et al., 2020; Elhadj Sidi et al., 2016; Sukumaran and Sudhakar, 2017; Ahmed et al., 2021; Mensah et al., 2019; Aslam et al., 2021; Malvoni et al., 2017; Banda et al., 2019; Chokmaviroj et al., 2006; Silva et al., 2020; Satish et al., 2020; Sharma and Chandel, 2013; Kymakis et al., 2009; Wittkopf et al., 2012; Phap and Nga, 2020; Drif et al., 2007; Sahouane et al., 2019; Al-Badi, 2020; Emmanuel et al., 2017; Atsu et al., 2021; Mi et al., 2016; Dondariya et al., 2018; Wu et al., 2015; Piao et al., 2009; Ameur et al., 2019; Haibaoui et al., 2017; Milosavljevic et al., 2015; Rout and Kulkarni, 2020; Ayompe et al., 2011; Karna et al., Jan. 2023; Emziane and Al Ali, 2015; Falih et al., 2022; Mohamed et al., 2024; Ates, 2023; Vidal et al., 2020; De Miguel et al., 2002; Owolabi et al., 2022; Seme et al., 2019; Piliougine et al., 2013; Guerra et al., 2017; Yakubu et al., 2024)

Table B
Performance ratio and Final yield values for each of the references analysed

Ref.	Year	Location	Type	Peak Power (P_0)	Performance Ratio (%)	Final yield (h/d)
(Iftikhar et al., 2021)	2021	Pakistan	On-Grid. Ground Utility scale	18 MW	81.40	-
(Bansal et al., 2022a)	2022	India	On-Grid. Ground Utility scale	10 MW	73.94	4.70
(Heyine et al., 2022)	2022	Mauritania	On-Grid. Utility scale	50 MW	73.34	5.87
(Maurya et al., 2022)	2022	India	On-Grid. Rooftop	40 kW	79.00	3.41
(K et al., 2018)	2018	India	On-Grid. Rooftop	40 kW	63.00	
(Haffaf et al., 2021)	2021	France	On-Grid. Rooftop	2.4 kW	-	3.75
(El Hacen Jed et al., 2020)	2020	Mauritania	On-Grid. Ground Utility scale	950 kW	66.00	2.41
(Bouacha et al., 2020)	2020	Algeria	On-Grid. Rooftop	9.5 kW	70.00	3.37
(Sharma and Goel, 2017)	2017	India	On-Grid. Rooftop	11.2 kW	78.00	3.67
(Yadav and Bajpai, 2018)	2018	India	On-Grid. Rooftop	5 kW	76.97	3.99
(Attari et al., 2016)	2016	Morocco	On-Grid. Rooftop	5 kW	79.00	4.45
(Thotakura et al., 2020)	2020	India	On-Grid. Rooftop Utility Scale	1 MW	88.00	4.60
(Okello et al., 2015)	2015	África	On-Grid. Rooftop	3.2 kW	84.30	4.90
(Al-Otaibi et al., 2015)	2015	Kuwait	On-Grid. Rooftop	106.6 kW	-	4.50
(Narasimman et al., 2023)	2023	India	On-Grid. Ground Utility scale	5 MW	44.00	-
(Mpholo et al., 2015)	2014	Lesotho	On-Grid. Ground Utility scale	281 kW	67.00	4.17
(Daher et al., 2018)	2018	Yubiti	On-Grid. Ground	302.4 kW	87.00	4.70
(Shuvho et al., 2019)	2019	Bangladesh	On-Grid. Rooftop	80 kW	66.00	2.53
(Chandel and Chandel, 2022)	2022	India	On-Grid. Ground Utility scale	19 MW	79.00	4.58
(Bentouba et al., 2021)	2021	Algeria	On-Grid. Ground Utility scale	20 MW	74.60	4.99
(Akhter et al., 2020)	2020	Malaysia	On-Grid. Rooftop	6.575 kW	81.60	2.99
(Oloya et al., 2021)	2021	Uganda	On-Grid. Ground Utility scale	10 MW	75.84	4.58
(Minai et al., 2022)	2022	India	On-Grid. Rooftop	467.2 kW	81.47	-
(Shiva Kumar and Sudhakar, 2015)	2021	India	On-Grid. Rooftop	100 kW	80.72	4.03
(Dobaria et al., 2016)	2016	India	On-Grid. Rooftop	5.05 kW	74.00	4.49
(Mukherji et al., 2020)	2019	India	On-Grid. Rooftop	50 kW	70.00	3.50
(Bansal et al., 2022b)	2022	India	On-Grid. Ground Utility scale	9 MW	70.76	4.40
(Sidrach-De-Cardona and López, 1998)	1998	Spain	On-Grid. Rooftop	2 kW	64.50	-
(Fuster-Palop et al., 2022)	2022	Spain	On-Grid. Ground Utility scale	50 MW	79.24	4.28
(Martín-Martínez et al., 2019)	2019	Spain	On-Grid. Ground Utility scale	2.7 MW	82.03	6.14
(Martín-Martínez et al., 2019)	2019	Spain	On-Grid. Ground Utility scale	1.4 MW	85.09	6.16
(Martín-Martínez et al., 2019)	2019	Spain	On-Grid. Ground Utility scale	370 kW	81.91	4.16
(Martín-Martínez et al., 2019)	2019	Spain	On-Grid. Ground Utility scale	1.3 MW	78.05	5.31
(Martín-Martínez et al., 2019)	2019	Spain	On-Grid. Ground Utility scale	1.3 MW	67.77	5.29
(Martín-Martínez et al., 2019)	2019	Spain	On-Grid. Ground Utility scale	4.6 MW	75.63	4.17
(Ayora et al., 2023)	2023	Kenya	On-Grid. Rooftop	600 kW	57.40	3.37
(Muñoz-Rodríguez et al., 2023)	2023	Spain	On-Grid. Rooftop	2.97 kW	83.00	4.38
(Abdullah and Nishimura, 2021)	2021	Japan	On-Grid. Rooftop	40.1 kW	68.10	2.59
(Roy et al., 2021)	2021	United Arab Emirates	On-Grid. Ground Utility scale	18 MW	74.10	-
(Castrillón-Mendoza et al., 2020)	2020	Colombia	On-Grid. Rooftop	152 kW	77.02	3.47
(Castrillón-Mendoza et al., 2020)	2020	Colombia	On-Grid. Rooftop	248 kW	74.60	3.42
(Jed et al., 2021)	2021	France	On-Grid. Ground Utility scale	4.5 MW	87.18	2.99
(Boddapati et al., 2021)	2019	India	On-Grid. Ground Utility scale	50 MW	77.90	-
(Dahmoun et al., 2021)	2017–2020	Algeria	On-Grid. Ground Utility scale	23.92 MW	82.00	4.95
(Sreenath et al., 2020)	2020	Malaysia	On-Grid. Ground Utility scale	20 MW	76.80	4.19
(Elhadj Sidi et al., 2016)	2015	Mauritania	On-Grid. Ground Utility scale	15 MW	67.90	4.27
(Sukumaran and Sudhakar, 2017)	2016	India	On-Grid. Ground Utility scale	12 MW	86.50	4.07

(continued on next page)

Table B (*continued*)

Ref.	Year	Location	Type	Peak Power (P_0)	Performance Ratio (%)	Final yield (h/d)
(Shiva Kumar and Sudhakar, 2015)	2015	India	On-Grid. Ground Utility scale	10 MW	85.12	-
(Ahmed et al., 2021)		Pakistan	On-Grid. Ground Utility scale	2.5 MW	80.50	4.49
(Mensah et al., 2019)	2013–2016	Ghana	On-Grid. Ground Utility scale	2.5 MW	70.60	-
(Aslam et al., 2021)	2020	Pakistan	On-Grid. Ground Utility scale	1 MW	76.50	3.90
(Malvoni et al., 2017)	2012–2015	Italy	On-Grid. Ground	960 kW	84.40	3.80
(Banda et al., 2019)	2013–2017	Malawi	On-Grid. Ground	830 kW	79.50	4.25
(Chokmaviroj et al., 2006)	2004	Thailand	On-Grid. Ground	500 kW	70.00	2.90
(Silva et al., 2020)	2019	Brazil	On-Grid. Rooftop	336.96 kW	83.50	-
(Satish et al., 2020)	2019	Dubai	On-Grid. Rooftop	200 kW	81.70	4.82
(Sharma and Chandel, 2013)	2011	India	On-Grid. Ground	190 kW	74.00	2.23
(Kymakis et al., 2009)	2007	Greece	On-Grid. Ground	171.36 kW	67.36	1.96
(Wittkopf et al., 2012)	2011	Singapore	On-Grid. Rooftop	142.5 kW	81.00	3.12
(Phap and Nga, 2020)	2019	Vietnam	On-Grid. Rooftop	56.7 kW	82.40	3.32
(Drif et al., 2007)	2003	Spain	On-Grid. Rooftop	40 kW	49.00	1.60
(Drif et al., 2007)	2003	Spain	On-Grid. Rooftop	67.84 kW	65.00	2.74
(Drif et al., 2007)	2003	Spain	On-Grid. Rooftop	67.84 kW	58.00	2.32
(Drif et al., 2007)	2003	Spain	On-Grid. Rooftop	20 kW	65.00	2.74
(Sahouane et al., 2019)	2017–2018	Africa	On-Grid. Rooftop	28 kW	71.89	4.40
(Al-Badi, 2020)	2014–2018	India	On-Grid. Rooftop	20.4 kW	67.00	3.64
(Emmanuel et al., 2017)	2014	New Zealand	On-Grid. Rooftop	10 kW	78.00	2.99
(Atsu et al., 2021)	2016	Hungary	On-Grid. Rooftop	9.6 kW	77.22	3.07
(Mi et al., 2016)	2015	China	On-Grid. Ground	9 kW	79.70	3.10
(Dondariya et al., 2018)	2018	India	On-Grid. Rooftop	6.4 kW	75.00	-
(Wu et al., 2015)	2009	China	On-Grid. Rooftop	3 kW	80.66	2.86
(Piao et al., 2009)	2003	Korea	On-Grid. Rooftop	3 kW	72.00	2.92
(Ameur et al., 2019)	2016	Morocco	On-Grid. Rooftop	2.4 kW	76.80	4.33
(Haibaoui et al., 2017)	2015	Morocco	On-Grid. Rooftop	5.94 kW	75.60	4.47
(Milosavljević et al., 2015)	2013	Serbia	On-Grid. Rooftop	2 kW	93.60	2.41
(Rout and Kulkarni, 2020)	2019	India	On-Grid. Rooftop	2 kW	70.00	-
(Ayompe et al., 2011)	2009	Ireland	On-Grid. Rooftop	1.72 kW	81.50	2.41
(Falih et al., 2022)	-	Iraq	On-Grid. Rooftop	5 kW	65.40	3.99
(Mohamed et al., 2024)	2022	Maldives	On-Grid. Rooftop	6.6 kW	69.37	3.87
(Ateş, 2023)	2018–2020	Turkey	On-Grid. Rooftop	30 kW	87.08	4.22
(Vidal et al., 2020)	2018	Chile	On-Grid. Ground	8.2 kW	85.50	3.60
(De Miguel et al., 2002)	2001	Spain	On-Grid. Rooftop	4.3 kW	69.80	3.23
(Owolabi et al., 2022)	2021	South Korea	On-Grid. Rooftop	5 kW	92.90	5.23
(Owolabi et al., 2022)	2021	South Korea	On-Grid. Rooftop	4.6 kW	93.50	4.93
(Seme et al., 2019)	2011–2018	Slovenia	On-Grid. Rooftop	111.8 kW	77.97	3.37
(Seme et al., 2019)	2011–2018	Slovenia	On-Grid. Rooftop	5.5 kW	49.59	2.31
(Seme et al., 2019)	2011–2018	Slovenia	On-Grid. Rooftop	47.9 kW	59.28	2.77
(Seme et al., 2019)	2011–2018	Slovenia	On-Grid. Rooftop	12.5 kW	84.53	3.5
(Seme et al., 2019)	2011–2018	Slovenia	On-Grid. Rooftop	7.1 kW	76.87	3.26
(Seme et al., 2019)	2011–2018	Slovenia	On-Grid. Rooftop	58.8 kW	70.81	3
(Seme et al., 2019)	2011–2018	Slovenia	On-Grid. Rooftop	71.4 kW	84.12	3.05
(Seme et al., 2019)	2011–2018	Slovenia	On-Grid. Rooftop	4.2 kW	67.78	3.17
(Seme et al., 2019)	2011–2018	Slovenia	On-Grid. Rooftop	77.4 kW	59.73	2.96
(Seme et al., 2019)	2011–2018	Slovenia	On-Grid. Rooftop	335 kW	82.74	3.04
(Seme et al., 2019)	2011–2018	Slovenia	On-Grid. Rooftop	19 kW	73.89	2.98
(Seme et al., 2019)	2011–2018	Slovenia	On-Grid. Rooftop	26.3 kW	69.91	2.76
(Seme et al., 2019)	2011–2018	Slovenia	On-Grid. Rooftop	14.7 kW	68.69	3.08
(Seme et al., 2019)	2011–2018	Slovenia	On-Grid. Rooftop	66.5 kW	76.65	3.42
(Piliougine et al., 2013)	2013	Spain	On-Grid. Rooftop	1.17 kW	94.1	5.3
(Guerra et al., 2017)	2013–2015	Spain	On-Grid. Rooftop	1.25 kW	78.6	3.95
(Guerra et al., 2017)	2013–2015	Spain	On-Grid. Rooftop	1.1 kW	80.76	4.12
(Yakubu et al., 2024)	2022	Ghana	On-Grid. Ground	50.76 kW	92.4	4.18

Data availability

The data that has been used is confidential.

References

Abdullah, G., Nishimura, H., 2021. Techno-economic performance analysis of a 40.1 kWp Grid-Connected Photovoltaic (GCPV) SYstem after Eight Years of Energy Generation: a Case Study for Tochigi, Japan. Sustainability 13 (14), 7680. https://doi.org/10.3390/su13147680.

Ahmed, N., Naveed Khan, A., Ahmed, N., Aslam, A., Imran, K., Sajid, M.B., Waqas, A., et al., 2021. Techno-economic potential assessment of mega scale grid-connected PV power plant in five climate zones of Pakistan. Energy Convers. Manag 237, 114097. https://doi.org/10.1016/J.ENCONMAN.2021.114097.

Akhter, M.N., Mekhilef, S., Mokhlis, H., Olatomiwa, L., Muhammad, M.A., 2020. Performance assessment of three grid-connected photovoltaic systems with combined capacity of 6.575 kWp in Malaysia (Dec.). J. Clean. Prod. 277, 123242. https://doi.org/10.1016/J.JCLEPRO.2020.123242.

Al-Aboosi, F.Y., Al-Aboosi, A.F., 2021. Preliminary evaluation of a rooftop grid-connected photovoltaic system installation under the climatic conditions of Texas (USA). Energies 14 (3). https://doi.org/10.3390/en14030586.

Al-Badi, A., 2020. Performance assessment of 20.4 kW eco-house grid-connected PV plant in Oman. Int. J. Sustain. Eng. 13 (3), 230–241. https://doi.org/10.1080/19397038.2019.1658824.

Ali, H., Khan, H.A., 2020. Analysis on inverter selection for domestic rooftop solar photovoltaic system deployment. Int. Trans. Electr. Energy Syst. 30 (5). https://doi.org/10.1002/2050-7038.12351.
Al-Otaibi, A., Al-Qattan, A., Fairouz, F., Al-Mulla, A., 2015. Performance evaluation of photovoltaic systems on Kuwaiti schools' rooftop. Energy Convers. Manag 95, 110–119. https://doi.org/10.1016/J.ENCONMAN.2015.02.039.
Ameur, A., Sekkat, A., Loudiyi, K., Aggour, M., 2019. Performance evaluation of different photovoltaic technologies in the region of Ifrane, Morocco. Energy Sustain. Dev. 52, 96–103. https://doi.org/10.1016/J.ESD.2019.07.007.
APPA Renovables, 2022. I Informe Anual del Autoconsumo Fotovoltaico.
APPA Renovables, "Informe Anual del Autoconsumo Fotovoltaico," Madrid, Feb. 2024.
A. Aslam, A.N. Khan, N. Ahmed, N. Ahmed, K. Imran, and M. Mahmood, "Effect of fixed and seasonal tilt angles on the performance of an ON-Grid PV plant," 2021 International Conference on Emerging Power Technologies, ICEPT 2021, Apr. 2021, doi: 10.1109/ICEPT51706.2021.9435464.
Ateş, A.M., 2023. 3-years energetic and economic analysis of a 30kWp Rooftop PV power plant. MüHend. ve Makina 64 (710), 175–194. https://doi.org/10.46399/MUHENDISMAKINA.1072368.
Atsu, D., Seres, I., Farkas, I., 2021. The state of solar PV and performance analysis of different PV technologies grid-connected installations in Hungary. Renew. Sustain. Energy Rev. 141, 110808. https://doi.org/10.1016/J.RSER.2021.110808.
Attari, K., Elyaakoubi, A., Asselman, A., 2016. Performance analysis and investigation of a grid-connected photovoltaic installation in Morocco. Energy Rep. 2, 261–266. https://doi.org/10.1016/J.EGYR.2016.10.004.
Ayompe, L.M., Duffy, A., McCormack, S.J., Conlon, M., 2011. Measured performance of a 1.72 kW rooftop grid connected photovoltaic system in Ireland. Energy Convers. Manag 52 (2), 816–825. https://doi.org/10.1016/J.ENCONMAN.2010.08.007.
Ayora, E., Munji, M., Kaberere, K., Thomas, B., 2023. Performance analysis of 600 kWp grid-tied rooftop solar photovoltaic systems at strathmore university in Kenya. Results Eng. 19, 101302. https://doi.org/10.1016/J.RINENG.2023.101302.
S. Bahari, M.J.A. Boushehri, and S. Sharifi, "Optimal Operation of Smart Grids in the Presence of Photovoltaic Units," 2023 13th Smart Grid Conference, SGC 2023, pp. 1–5, Dec. 2023, doi: 10.1109/SGC61621.2023.10459312.
Banda, M.H., Nyeinga, K., Okello, D., 2019. Performance evaluation of 830 kWp grid-connected photovoltaic power plant at Kamuzu International Airport-Malawi. Energy Sustain. Dev. 51, 50–55. https://doi.org/10.1016/J.ESD.2019.05.005.
Bansal, N., Jaiswal, S.P., Singh, G., 2022a. Long term operational performance and experimental on-field degradation measurement of 10 MW PV plant in remote location in India. Energy Sustain. Dev. 67, 135–150. https://doi.org/10.1016/J.ESD.2022.01.007.
Bansal, N., Jaiswal, S.P., Singh, G., 2022b. Long term performance assessment and loss analysis of 9 MW grid tied PV plant in India. Mater. Today Proc. 60, 1056–1067. https://doi.org/10.1016/J.MATPR.2022.01.263.
Bennouna, A., Aarich, N., Erraissi, N., Akhsassi, M., Asselman, A., Barhdadi, A., et al., 2019. Energy performance of 3 silicon-based PV module technologies in 20 sites of Morocco. Energy Sustain. Dev. 53, 30–56. https://doi.org/10.1016/J.ESD.2019.09.002.
Bentouba, S., Bourouis, M., Zioui, N., Pirashanthan, A., Velauthapillai, D., 2021. Performance assessment of a 20 MW photovoltaic power plant in a hot climate using real data and simulation tools. Energy Rep. 7, 7297–7314. https://doi.org/10.1016/J.EGYR.2021.10.082.
Berastain, A.E., Conde, L.A., Angulo, J., Carhuavilca, A.M., García, M., Sevillano-Bendezú, M.A., et al., 2022. Resolving challenges of monitoring PV systems: A case study for three 1.5 kW generators in Lima, Peru. Journal of Physics: Conference Series. IOP Publishing Ltd. https://doi.org/10.1088/1742-6596/2180/1/012006.
Boddapati, V., Nandikatti, A.S.R., Daniel, S.A., 2021. Techno-economic performance assessment and the effect of power evacuation curtailment of a 50 MWp grid-interactive solar power park. Energy Sustain. Dev. 62, 16–28. https://doi.org/10.1016/J.ESD.2021.03.005.
Borah, P., Micheli, L., Sarmah, N., 2023. Analysis of soiling loss in photovoltaic modules: a review of the impact of atmospheric parameters, soil properties, and mitigation approaches. Sustainability 15 (24), 16669.
Bouacha, S., Malek, A., Benkraouda, O., Arab, A.H., Razagui, A., Boulahchiche, S., et al., 2020. Performance analysis of the first photovoltaic grid-connected system in Algeria. Energy Sustain. Dev. 57, 1–11. https://doi.org/10.1016/J.ESD.2020.04.002.
Castrillón-Mendoza, R., Manrique-Castillo, P.A., Rey-Hernández, J.M., Rey-Martínez, F. J., González-Palomino, G., 2020. PV energy performance in a sustainable campus. Electronics 9 (11), 1874. https://doi.org/10.3390/electronics9111874.
Chandel, R., Chandel, S.S., 2022. Performance analysis outcome of a 19-MWp commercial solar photovoltaic plant with fixed-tilt, adjustable-tilt, and solar tracking configurations. Prog. Photovolt. Res. Appl. 30 (1), 27–48. https://doi.org/10.1002/pip.3458.
Chokmaviroj, S., Wattanapong, R., Suchart, Y., 2006. Performance of a 500 kWP grid connected photovoltaic system at Mae Hong Son Province, Thailand. Renew. Energy 31 (1), 19–28. https://doi.org/10.1016/J.RENENE.2005.03.004.
Dabou, R., Bouchafaa, F., Arab, A.H., Bouraiou, A., Draou, M.D., Neçaibia, A., et al., 2016. Monitoring and performance analysis of grid connected photovoltaic under different climatic conditions in south Algeria. Energy Convers. Manag 130, 200–206. https://doi.org/10.1016/J.ENCONMAN.2016.10.058.
Daher, D.H., Gaillard, L., Amara, M., Ménézo, C., 2018. Impact of tropical desert maritime climate on the performance of a PV grid-connected power plant. Renew. Energy 125, 729–737. https://doi.org/10.1016/J.RENENE.2018.03.013.
Dahmoun, M.E.H., Bekkouche, B., Sudhakar, K., Guezgouz, M., Chenafi, A., Chaouch, A., 2021. Performance evaluation and analysis of grid-tied large scale PV plant in Algeria. Energy Sustain. Dev. 61, 181–195. https://doi.org/10.1016/J.ESD.2021.02.004.
A. De Miguel, J. Bilbao, J.R.S. Cazorro, and C. Martín, Performance analysis of a grid-connected PV system in a rural site in the Northwest of Spain. 2002.
Desai, A., Mukhopadhyay, I., Ray, A., 2020. Performance analysis of string and central inverter based ideally designed utility scale solar PV plant. Conf. Rec. IEEE Photovolt. Spec. Conf. 2020-June, 2412–2417. https://doi.org/10.1109/PVSC45281.2020.9300494.
Díez-Mediavilla, M., Dieste-Velasco, M.I., Rodríguez-Amigo, M.C., García-Calderón, T., Alonso-Tristán, C., 2014. Performance of grid-tied PV facilities based on real data in Spain: central inverter versus string system. Energy Convers. Manag 86. https://doi.org/10.1016/j.enconman.2014.06.087.
Dobaria, B., Pandya, M., Aware, M., 2016. Analytical assessment of 5.05 kWp grid tied photovoltaic plant performance on the system level in a composite climate of western India. Energy 111, 47–51. https://doi.org/10.1016/J.ENERGY.2016.05.082.
Dogga, R., Pathak, M.K., 2019. Recent trends in solar PV inverter topologies. Sol. Energy 183, 57–73. https://doi.org/10.1016/J.SOLENER.2019.02.065.
Dondariya, C., Porwal, D., Awasthi, A., Shukla, A.K., Sudhakar, K., Murali, M.M., et al., 2018. Performance simulation of grid-connected rooftop solar PV system for small households: a case study of Ujjain, India. Energy Rep. 4, 546–553. https://doi.org/10.1016/J.EGYR.2018.08.002.
Drif, M., Pérez, P.J., Aguilera, J., Almonacid, G., Gomez, P., de la Casa, J., et al., 2007. Univer Project. A grid connected photovoltaic system of 200kWp at Jaén University. Overview and performance analysis. Sol. Energy Mater. Sol. Cells 91 (8), 670–683. https://doi.org/10.1016/J.SOLMAT.2006.12.006.
El Hacen Jed, M., Ihaddadene, R., Ihaddadene, N., Elhadji Sidi, C.Elb, EL Bah, M., 2020. Performance analysis of 954,809 kWp PV array of Sheikh Zayed solar power plant (Nouakchott, Mauritania). Renew. Energy Focus 32, 45–54. https://doi.org/10.1016/J.REF.2019.11.002.
Elhadj Sidi, C.E.B., Ndiaye, M.L., El Bah, M., Mbodji, A., Ndiaye, A., Ndiaye, P.A., 2016. Performance analysis of the first large-scale (15 MWp) grid-connected photovoltaic plant in Mauritania. Energy Convers. Manag 119, 411–421. https://doi.org/10.1016/J.ENCONMAN.2016.04.070.
Emmanuel, M., Akinyele, D., Rayudu, R., 2017. Techno-economic analysis of a 10 kWp utility interactive photovoltaic system at Maungaraki school, Wellington, New Zealand. Energy 120, 573–583. https://doi.org/10.1016/J.ENERGY.2016.11.107.
Emziane, M., Al Ali, M., 2015. Performance assessment of rooftop PV systems in Abu Dhabi. Energy Build. 108, 101–105. https://doi.org/10.1016/J.ENBUILD.2015.08.057.
Falih, H., J. Hamed, A., Khalifa, A.H.N., 2022. Performance analysis of a rooftop hybrid connected solar PV system. Energy Eng. 119 (4), 1729–1744. https://doi.org/10.32604/EE.2022.021190.
Farahmand, M.Z., Nazari, M.E., Shamlou, S., Shafie-Khah, M., 2021. The simultaneous impacts of seasonal weather and solar conditions on PV panels electrical characteristics. Energies 14 (4), 845. https://doi.org/10.3390/EN14040845.
Fassbender, E., Rott, J., Hemmerle, C., 2024. Impacts of Photovoltaic Façades on the Urban Thermal microclimate and outdoor thermal comfort: simulation-based analysis. Buildings 14 (4), 923. https://doi.org/10.3390/BUILDINGS14040923.
Fuster-Palop, E., Vargas-Salgado, C., Ferri-Revert, J.C., Payá, J., 2022. Performance analysis and modelling of a 50 MW grid-connected photovoltaic plant in Spain after 12 years of operation. Renew. Sustain. Energy Rev. 170, 112968. https://doi.org/10.1016/J.RSER.2022.112968.
García, J.L., Perdigones, A., Benavente, R.M., Álvarez, J., Baptista, F., Mazarrón, F.R., 2023. Feasibility of photovoltaic systems for the agrifood industry in the new energy and climate change context. Agronomy 13 (10), 2620. https://doi.org/10.3390/AGRONOMY13102620.
Gergely, L.Z., Csoknyai, T., Horváth, M., 2022. Novel load matching indicators for photovoltaic system sizing and evaluation. Appl. Energy 327, 120123. https://doi.org/10.1016/J.APENERGY.2022.120123.
González-González, E., Martín-Jiménez, J., Sánchez-Aparicio, M., Del Pozo, S., Lagüela, S., 2022. Evaluating the standards for solar PV installations in the Iberian Peninsula: Analysis of tilt angles and determination of solar climate zones. Sustain. Energy Technol. Assess. 49, 101684. https://doi.org/10.1016/J.SETA.2021.101684.
Guerra, T.A., Guerra, J.A., Tabernero, B.O., De La Cruz García, G., 2017. Comparative energy performance analysis of six primary photovoltaic technologies in Madrid (Spain). Energies 10 (6), 772. https://doi.org/10.3390/EN10060772.
Haffaf, A., Lakdja, F., Ould Abdeslam, D., Meziane, R., 2021b. Monitoring, measured and simulated performance analysis of a 2.4 kWp grid-connected PV system installed on the Mulhouse campus, France. Energy Sustain. Dev. 62, 44–55. https://doi.org/10.1016/J.ESD.2021.03.006.
Haibaoui, A., Hartiti, B., Elamim, A., Karami, M., Ridah, A., 2017. Performance indicators for grid-connected PV systems: a case study In Casablanca, Morocco. IOSR J. Electr. Electron. Eng. 12 (02), 55–65. https://doi.org/10.9790/1676-1202015565.
Heyine, M.S., Yahya, A.M., Daher, D.H., Gaillard, L., Menezo, C., Mahmoud, A.K., 2022. Performance evaluation of 50MWp solar plant under different climatic conditions. Int. J. Power Electron. Drive Syst. 13 (1), 561–575. https://doi.org/10.11591/ijpeds.v13.i1.pp561-575.
Iftikhar, H., Sarquis, E., Costa Branco, P.J., 2021. Why can simple operation and maintenance (O&m) practices in large-scale grid-connected pv power plants play a key role in improving its energy output? Energies 14 (13). https://doi.org/10.3390/en14133798.
International Energy Agency, "Electricity 2024 - Analysis and forecast to 2026," Paris, Jan. 2024a.
International Energy Agency, "Snapshot of Global PV Markets 2024," Paris, Apr. 2024b.

International Energy Agency, "World Energy Outlook 2023," Paris, Oct. 2023.
ISO/IEC, "61724-1:2022 Photovoltaic system performance - Part 1: Monitoring," 2022.
ISO/IEC, "61724-2:2016 Photovoltaic system performance - Part 2: Capacity evaluation method," 2016a.
ISO/IEC, "61724-3:2016 Photovoltaic system performance - Part 3: Energy evaluation method," 2016b.
Jed, M.E.H., Logerais, P.-O., Malye, C., Riou, O., Delaleux, F., El Bah, M., 2021. Analysis of the performance of the photovoltaic power plant of Sourdun (France). Int. J. Sustain. Eng. 14 (6), 1756–1768. https://doi.org/10.1080/19397038.2021.1971321.
Jianxun, W., Xin, C., Weicheng, J., Li, H., Junyi, L., Haigang, S., 2023. PVNet: A novel semantic segmentation model for extracting high-quality photovoltaic panels in large-scale systems from high-resolution remote sensing imagery. Int. J. Appl. Earth Obs. Geoinf. 119, 103309. https://doi.org/10.1016/J.JAG.2023.103309.
Jiménez-Castillo, G., Martínez-Calahorro, A.J., Rus-Casas, C., Benítez-Andrades, J.A., Muñoz-Rodriguez, F.J., 2023. Rooftop Solar Photovoltaic Systems for Building of Industrial. Springe Proc. Earth Environ. Sci. Part F639, 414–422. https://doi.org/10.1007/978-3-031-25840-4_48.
Jimenez-Castillo, G., Martinez-Calahorro, A.J., Rus-Casas, C., Snytko, A., Munoz-Rodriguez, F.J., 2023. Performance analysis indices for Rooftop Solar Photovoltaic system. IEEE Lat. Am. Trans. 21 (9), 999–1006. https://doi.org/10.1109/TLA.2023.10251806.
G. Jiménez-Castillo, J.L. Sánchez Jiménez, J.I.F. Carrasco, C. Rus-Casas, J.C. Hernandez, and F. Muñoz-Rodriguez, "Analysing the Performance of Electricity Generation through PV Rooftop Systems in Food Industry Facilities," in VII Ibero-American Congress of Smart Cities (ICSC-CITIES 2024), San Carlos, Costa Rica, Nov. 2024, pp. 464–476.
Muñoz-Rodríguez, F.J., Snytko, A., de la Casa Hernández, J., Rus-Casas, C., Jiménez-Castillo, G., 2023. Rooftop photovoltaic systems. New parameters for the performance analysis from monitored data based on IEC 61724. Energy Build. 295, 113280. https://doi.org/10.1016/J.ENBUILD.2023.113280.
Karna, S.L., Jha, A.K., Yadav, K., Kumar Mallik, J., Jan. 2023. Performance evaluation of solar PV mini grid system in Nepal: a case study Thabang and Sugarkhal. Front Energy Res 11, 1321945. https://doi.org/10.3389/FENRG.2023.1321945/BIBTEX.
Kumar, N.M., Yadav, S.K., Chopra, S.S., Bajpai, U., Gupta, R.P., Padmanaban, S., et al., 2020. Operational performance of on-grid solar photovoltaic system integrated into pre-fabricated portable cabin buildings in warm and temperate climates. Energy Sustain. Dev. 57, 109–118. https://doi.org/10.1016/J.ESD.2020.05.008.
Kurtz, S., Newmiller, J., Kimber, A., Flottemesch, R., Riley, E., Dierauf, T., et al., 2013. Analysis of photovoltaic system energy performance evaluation method. Natl. Renew. Energy Lab.
Kymakis, E., Kalykakis, S., Papazoglou, T.M., 2009. Performance analysis of a grid connected photovoltaic park on the island of Crete. Energy Convers. Manag 50 (3), 433–438. https://doi.org/10.1016/J.ENCONMAN.2008.12.009.
Lagarde, Q., Beillard, B., Mazen, S., Denis, M.S., Leylavergne, J., 2023. Performance ratio of photovoltaic installations in France: Comparison between inverters and micro-inverters (Dec.). J. King Saud. Univ. Eng. Sci. 35 (8), 531–538. https://doi.org/10.1016/J.JKSUES.2021.11.007.
Lee, H., Choi, M., Kim, J., Kim, D., Bae, S., Yoon, J., 2023. Partial shading losses mitigation of a rooftop PV system with DC power optimizers based on operation and simulation-based evaluation. Sol. Energy 265, 112053. https://doi.org/10.1016/J.SOLENER.2023.112053.
Litjens, G.B.M.A., Worrell, E., van Sark, W.G.J.H.M., 2017. Influence of demand patterns on the optimal orientation of photovoltaic systems. Sol. Energy 155, 1002–1014. https://doi.org/10.1016/J.SOLENER.2017.07.006.
Malvoni, M., Leggieri, A., Maggiotto, G., Congedo, P.M., De Giorgi, M.G., 2017. Long term performance, losses and efficiency analysis of a 960 kWP photovoltaic system in the Mediterranean climate. Energy Convers. Manag 145, 169–181. https://doi.org/10.1016/J.ENCONMAN.2017.04.075.
A.J. Martinez Calahorro, G. Jimenez Castillo, C. Rus Casas, and F.J. Muñoz Rodriguez, "Distributed generation and photovoltaic self-consumption. energy potential for the olive mill industries in Spain," Dyna, vol. 95, no. 1, pp. 591–595, Nov. 2020, doi: 10.6036/9748.
Martín-Martínez, S., Cañas-Carretón, M., Honrubia-Escribano, A., Gómez-Lázaro, E., 2019. Performance evaluation of large solar photovoltaic power plants in Spain. Energy Convers. Manag 183, 515–528. https://doi.org/10.1016/J.ENCONMAN.2018.12.116.
A.K. Maurya, A. Kumar Rai, and H. Ahuja, "Performance Analysis of Roof-top Solar PV System in Composite Environment," in 2022 IEEE 10th Power India International Conference, PIICON 2022, Institute of Electrical and Electronics Engineers Inc., 2022. doi: 10.1109/PIICON56320.2022.10045154.
Mensah, L.D., Yamoah, J.O., Adaramola, M.S., 2019. Performance evaluation of a utility-scale grid-tied solar photovoltaic (PV) installation in Ghana. Energy Sustain. Dev. 48, 82–87. https://doi.org/10.1016/J.ESD.2018.11.003.
Mi, Z., Chen, J., Chen, N., Bai, Y., Wu, W., Fu, R., et al., 2016. Performance analysis of a grid-connected high concentrating photovoltaic system under practical operation conditions. Energies 9 (2), 117. https://doi.org/10.3390/EN9020117.
Milosavljević, D.D., Pavlović, T.M., Piršl, D.S., 2015. Performance analysis of A grid-connected solar PV plant in Niš, republic of Serbia. Renew. Sustain. Energy Rev. 44, 423–435. https://doi.org/10.1016/J.RSER.2014.12.031.
Minai, A.F., Usmani, T., Alotaibi, M.A., Malik, H., Nassar, M.E., 2022. Performance Analysis and Comparative Study of a 467.2 kWp Grid-Interactive SPV System: a case study. Energies 15 (3). https://doi.org/10.3390/en15031107.
Mohamed, K., Shareef, H., Nizam, I., Esan, A.B., Shareef, A., 2024. Operational performance assessment of rooftop PV Systems in the Maldives. Energy Rep. 11, 2592–2607. https://doi.org/10.1016/J.EGYR.2024.02.014.
Mohammed, A., Ghaithan, A., Al-Hanbali, A., Attia, A.M., Saleh, H., Alsawafy, O., 2022. Performance evaluation and feasibility analysis of 10 kWp PV system for residential buildings in Saudi Arabia. Sustain. Energy Technol. Assess. 51, 101920. https://doi.org/10.1016/J.SETA.2021.101920.
Montes, C., Dorta-Guerra, R., González-Díaz, B., González-Pérez, S., Ocaña, L., Llarena, E., 2022. Study of the evolution of the performance ratio of photovoltaic plants operating in a utility-scale installation located at a subtropical climate zone using mixed-effects linear modeling. Appl. Sci. 12 (21), 11306. https://doi.org/10.3390/app122111306.
Motahhir, S., Chouder, A., El Hammoumi, A., Benyoucef, A.S., El Ghzizal, A., Kichou, S., et al., 2020. Optimal energy harvesting from a multistrings PV generator based on artificial bee colony algorithm. IEEE Syst. J. 15 (3), 4137–4144. https://doi.org/10.1109/JSYST.2020.2997744.
Mpholo, M., Nchaba, T., Monese, M., 2015. Yield and performance analysis of the first grid-connected solar farm at Moshoeshoe I International Airport, Lesotho. Renew. Energy 81, 845–852. https://doi.org/10.1016/J.RENENE.2015.04.001.
Mukherji, R., Mathur, V., Bhati, A., Mukherji, M., 2020. Assessment of 50 kWp rooftop solar photovoltaic plant at The ICFAI University, Jaipur: a case study. Environ. Prog. Sustain Energy 39 (3). https://doi.org/10.1002/ep.13353.
Muñoz-Rodríguez, F.J., Gómez, P., Fernández-Carrasco, J.I., Tina, G.M., Jiménez-Castillo, G., 2025. A new approach to analyse from monitored data the performance, matching capability and grid usage of large Rooftop Photovoltaic systems. Case of study: Photovoltaic system of 1.05 MW installed at the campus of University of Jaén. Renew. Energy 239, 121947. https://doi.org/10.1016/j.renene.2024.121947.
Narasimman, K., Gopalan, V., Bakthavatsalam, A.K., Elumalai, P.V., Iqbal Shajahan, M., Joe Michael, J., 2023. Modelling and real time performance evaluation of a 5 MW grid-connected solar photovoltaic plant using different artificial neural networks. Energy Convers. Manag 279, 116767. https://doi.org/10.1016/J.ENCONMAN.2023.116767.
Ocampo, E.M., Chang, W.C., Kuo, C.C., 2021. Optimal Sizing of PV-Diesel-Battery System Using Different Inverter Types. IEEE Access 9, 133561–133573. https://doi.org/10.1109/ACCESS.2021.3114763.
E. Ogliari, S. Leva, M. Polenghi, and L. De Ciechi, "Comparative Performance analysis of different PV plants in Italy," Proceedings - 2023 IEEE International Conference on Environment and Electrical Engineering and 2023 IEEE Industrial and Commercial Power Systems Europe, EEEIC / I and CPS Europe 2023, Jun. 2023, doi: 10.1109/EEEIC/ICPSEUROPE57605.2023.10194655.
Okello, D., Van Dyk, E.E., Vorster, F.J., 2015. Analysis of measured and simulated performance data of a 3.2 kWp grid-connected PV system in Port Elizabeth, South Africa. Energy Convers. Manag 100, 10–15. https://doi.org/10.1016/J.ENCONMAN.2015.04.064.
Oloya, I.T., Gutu, T.J.L., Adaramola, M.S., 2021. Techno-economic assessment of 10 MW centralised grid-tied solar photovoltaic system in Uganda. Case Stud. Therm. Eng. 25, 100928. https://doi.org/10.1016/J.CSITE.2021.100928.
Ordóñez, J., Jadraque, E., Alegre, J., Martínez, G., 2010. Analysis of the photovoltaic solar energy capacity of residential rooftops in Andalusia (Spain). Renew. Sustain. Energy Rev. 14 (7), 2122–2130. https://doi.org/10.1016/J.RSER.2010.01.001.
Owolabi, A.B., Yakub, A.O., Li, H.X., Suh, D., 2022. Performance evaluation of two grid-connected solar photovoltaic systems under temperate climatic conditions in South Korea. Energy Rep. 8, 12227–12236. https://doi.org/10.1016/J.EGYR.2022.09.053.
K, P.S., Das D, B., Sailesh, S.B., Saxena, A.K., 2018. Performance analysis of grid interactive solar photovoltaic plant in India (Dec.). Energy Sustain. Dev. 47, 9–16. https://doi.org/10.1016/J.ESD.2018.08.003.
Perdigones, A., García, J.L., García, I., Baptista, F., Mazarrón, F.R., 2023. Economic Feasibility of PV Mounting Structures on Industrial Roofs, 2023, Vol. 13, Page 2834 Buildings 13 (11), 2834. https://doi.org/10.3390/BUILDINGS13112834.
Phap, V.M., Nga, N.T., 2020. Feasibility study of rooftop photovoltaic power system for a research institute towards green building In Vietnam. EAI Endorsed Trans. Energy Web "7" (26). https://doi.org/10.4108/EAI.7-1-2020.162825.
Piao, Z.G., Jung, B.I., Choi, Y.O., Cho, G.B., 2009. Performance assessment of 3kW grid-connected PV systems in Korea. INTELEC Int. Telecommun. Energy Conf. https://doi.org/10.1109/INTLEC.2009.5351953.
Piliougine, M., Cañete, C., Moreno, R., Carretero, J., Hirose, J., Ogawa, S., et al., 2013. Comparative analysis of energy produced by photovoltaic modules with anti-soiling coated surface in arid climates. Appl. Energy 112, 626–634. https://doi.org/10.1016/J.APENERGY.2013.01.048.
Polleux, L., Guerassimoff, G., Marmorat, J.P., Sandoval-Moreno, J., Schuhler, T., 2022. An overview of the challenges of solar power integration in isolated industrial microgrids with reliability constraints. Renew. Sustain. Energy Rev. 155, 111955. https://doi.org/10.1016/J.RSER.2021.111955.
G.A. Puche, P.G. Vidal, and E. Muñoz-Cerón, "Large-Scale Photovoltaic Power Plants," pp. 125–169, Jun. 2016, doi: 10.1142/9789814689502_0004.
Rout, K.C., Kulkarni, P.S., 2020. Design and performance evaluation of Proposed 2 kW Solar PV Rooftop on Grid System in Odisha using PVsyst. 2020 IEEE International Students' Conference on Electrical, Electronics and Computer Science, SCEECS 2020. https://doi.org/10.1109/SCEECS48394.2020.124.
Roy, H.A., Alremeithi, A., Atyani, M., Farina, M., Alnuaimi, A., 2021. Field performance evaluation of the largest rooftop PV Project in the Middle East. IEEE 48th Photovoltaic Specialists Conference (PVSC), pp. 468–471. https://doi.org/10.1109/PVSC43889.2021.9518787.
Sahouane, N., Dabou, R., Ziane, A., Neçaibia, A., Bouraiou, A., Rouabhia, A., et al., 2019. Energy and economic efficiency performance assessment of a 28 kWp photovoltaic grid-connected system under desertic weather conditions in Algerian Sahara. Renew. Energy 143, 1318–1330. https://doi.org/10.1016/J.RENENE.2019.05.086.
Santiago, I., Trillo Montero, D., Luna Rodríguez, J.J., Moreno Garcia, I.M., Palacios Garcia, E.J., 2017. Graphical diagnosis of performances in photovoltaic systems: a

case study in southern Spain. Energ. (Basel) 10 (12). https://doi.org/10.3390/en10121964.
Santiago, I., Trillo-Montero, D., Moreno-Garcia, I.M., Pallarés-López, V., Luna-Rodríguez, J.J., 2018. Modeling of photovoltaic cell temperature losses: a review and a practice case in South Spain. Renew. Sustain. Energy Rev. 90, 70–89. https://doi.org/10.1016/J.RSER.2018.03.054.
Satish, M., Santhosh, S., Yadav, A., 2020. Simulation of a Dubai based 200 KW power plant using PVsyst software. 7th International Conference on Signal Processing and Integrated Networks, SPIN, 2020, pp. 824–827. https://doi.org/10.1109/SPIN48934.2020.9071135.
Schardt, J., te Heesen, H., 2021. Performance of roof-top PV systems in selected European countries from 2012 to 2019. Sol. Energy 217, 235–244. https://doi.org/10.1016/J.SOLENER.2021.02.001.
Seme, S., Sredenšek, K., Štumberger, B., Hadžiselimović, M., 2019. Analysis of the performance of photovoltaic systems in Slovenia. Sol. Energy 180, 550–558. https://doi.org/10.1016/J.SOLENER.2019.01.062.
Sharma, R., Goel, S., 2017. Performance analysis of a 11.2 kWp roof top grid-connected PV system in Eastern India. Energy Rep. 3, 76–84. https://doi.org/10.1016/J.EGYR.2017.05.001.
Sharma, V., Chandel, S.S., 2013. Performance analysis of a 190 kWp grid interactive solar photovoltaic power plant in India. Energy 55, 476–485. https://doi.org/10.1016/J.ENERGY.2013.03.075.
Shiva Kumar, B., Sudhakar, K., 2015. Performance evaluation of 10 MW grid connected solar photovoltaic power plant in India. Energy Rep. 1, 184–192. https://doi.org/10.1016/j.egyr.2015.10.001.
Shuvho, M.B.A., Chowdhury, M.A., Ahmed, S., Kashem, M.A., 2019. Prediction of solar irradiation and performance evaluation of grid connected solar 80KWp PV plant in Bangladesh. Energy Rep. 5, 714–722. https://doi.org/10.1016/J.EGYR.2019.06.011.
Sidrach-De-Cardona, M., López, L.M., 1998. Evaluation of a grid-connected photovoltaic system in southern Spain. Renew. Energy 15 (1–4), 527–530. https://doi.org/10.1016/S0960-1481(98)00218-3.
Silva, J.L.D.S., Costa, T.S., De Melo, K.B., Sako, E.Y., Moreira, H.S., Villalva, M.G., 2020. A comparative performance of PV power simulation software with an installed PV plant. Proc. IEEE Int. Conf. Ind. Technol. 2020-February, 531–535. https://doi.org/10.1109/ICIT45562.2020.9067138.
SolarPower Europe, "SolarPower Europe (2023): EU Market Outlook for Solar Power 2023-2027.," 2023.
Sreenath, S., Sudhakar, K., Yusop, A.F., Solomin, E., Kirpichnikova, I.M., 2020. Solar PV energy system in Malaysian airport: Glare analysis, general design and performance assessment. Energy Rep. 6, 698–712. https://doi.org/10.1016/J.EGYR.2020.03.015.
Srivastava, R., Tiwari, A.N., Giri, V.K., 2020. An overview on performance of PV plants commissioned at different places in the world. Energy Sustain. Dev. 54, 51–59. https://doi.org/10.1016/J.ESD.2019.10.004.
Sukumaran, S., Sudhakar, K., 2017. Fully solar powered airport: A case study of Cochin International airport. J. Air Transp. Manag 62, 176–188. https://doi.org/10.1016/J.JAIRTRAMAN.2017.04.004.
J. Taylor, R. Moretón, J. Leloux, L. Narvarte, D. Trebosc, and A. Desportes, "Monitoring 30,000 PV systems in Europe: Performance, Faults, and State of the Art," in 31st European Photovoltaic Solar Energy Conference and Exhibition, Hamburg, Germany, Sep. 2015, pp. 1574–1582.
Thotakura, S., Kondamudi, S.C., Xavier, J.F., Quanjin, M., Reddy, G.R., Gangwar, P., et al., 2020. Operational performance of megawatt-scale grid integrated rooftop solar PV system in tropical wet and dry climates of India. Case Stud. Therm. Eng. 18, 100602. https://doi.org/10.1016/J.CSITE.2020.100602.
Veerendra Kumar, D.J., Deville, L., Ritter, K.A., Raush, J.R., Ferdowsi, F., Gottumukkala, R., et al., 2022. Performance evaluation of 1.1 MW grid-connected solar photovoltaic power plant in Louisiana. Energies 15 (9). https://doi.org/10.3390/en15093420.
Vidal, H., Rivera, M., Wheeler, P., Vicencio, N., 2020. The analysis performance of a grid-connected 8.2 kWp photovoltaic system in the Patagonia region. Sustainability 12 (21), 9227. https://doi.org/10.3390/SU12219227.
Wittkopf, S., Valliappan, S., Liu, L., Ang, K.S., Cheng, S.C.J., 2012. Analytical performance monitoring of a 142.5 kWp grid-connected rooftop BIPV system in Singapore. Renew. Energy 47, 9–20. https://doi.org/10.1016/J.RENENE.2012.03.034.
Woyte, A., Richter, M., Moser, D., Green, M., Mau, S., Beyer, H.G., 2014. Analytical Monitoring of Grid-connected Photovoltaic Systems, vol. 13(2).
Wu, X., Liu, Y., Xu, J., Lei, W., Si, X., Du, W., et al., 2015. Monitoring the performance of the building attached photovoltaic (BAPV) system in Shanghai. Energy Build. 88, 174–182. https://doi.org/10.1016/J.ENBUILD.2014.11.073.
Yadav, S.K., Bajpai, U., 2018. Performance evaluation of a rooftop solar photovoltaic power plant in Northern India. Energy Sustain. Dev. 43, 130–138. https://doi.org/10.1016/J.ESD.2018.01.006.
Yakubu, R.O., Ijeoma, M.W., Yusuf, H., Abdulazeez, A.A., Acheampong, P., Carbajales-Dale, M., 2024. Performance analysis of a 50 MW solar PV installation at BUI power authority: a comparative study between sunny and overcast days. Electricity 5 (3), 546–561. https://doi.org/10.3390/ELECTRICITY5030027.
Zeb, K., Uddin, W., Khan, M.A., Ali, Z., Ali, M.U., Christofides, N., et al., 2018. A comprehensive review on inverter topologies and control strategies for grid connected photovoltaic system. Renew. Sustain. Energy Rev. 94, 1120–1141. https://doi.org/10.1016/J.RSER.2018.06.053.

Glossary

Photovoltaic (PV) System: A system that converts sunlight into electrical energy using solar panels and inverters.
Self-Consumption: The direct use of electricity generated by a PV system within the same facility where it is produced, reducing the need for grid-supplied power.
PV array energy yield (Y_A): The energy output (DC) per rated kilowatt (DC) of the installed PV array.
Final Yield (Y_f): The net energy output of the entire PV system (AC) per rated kilowatt (DC) of the installed PV array over a specific period.
Equivalent Capacity Utilisation Yield (Y_L): Defined as the total number of hours within the analysis period during which the instantaneous power demand equals the contracted power level or the capacity of the grid connection node.
Final self-consumption yield ($Y_{f,PVSC}$): Metric that indicate the self-consumed energy per kW.
Final to grid yield ($Y_{f,TG}$): Metric that indicate, if no storage system is considered, the energy that is not directly self-consumed and can be exported to the grid.
Load ratio yield (Y_{GL}): Metric that represents the hours of operation that the connection node is operating at maximum capacity.
Load ratio to grid yield ($Y_{GL,TG}$): Metric that represent the equivalent hours when the grid is operating at full capacity exporting to grid.
Load ratio from grid yield ($Y_{GL,FG}$): Metric that represent the equivalent hours when the grid is operating at full capacity importing from grid.
Performance Ratio (PR): A key metric for evaluating PV system efficiency, representing the ratio of actual energy output (Y_f) to the theoretical maximum energy output under ideal conditions (Y_r).
Capacity Utilization Factor (CUF): A measure of how efficiently a PV system operates compared to its maximum possible generation. Its calculation is based on the rated AC power ($P_{0,AC}$) of the system and defines the fraction of electrical energy generated compared to the energy that would have been generated by operating at 100 % of its rated AC power during the reporting period, typically 365 days.
Global Horizontal Irradiance (GHI): The total solar radiation received per unit area on a horizontal surface.
Capture losses (L_C): Energy losses due to shading, soiling, and other environmental factors that reduce the amount of solar radiation effectively converted into electricity.
Load ratio (GL): This parameter describes the amount of energy transferred at a given point in the grid without considering the direction of the flow
Inverter efficiency: The effectiveness of an inverter in converting direct current (DC) from PV modules into alternating current (AC) with minimal energy losses.
Maximum Power Point Tracking (MPPT): A control technique used in inverters to dynamically adjust the operating voltage of PV modules for maximum energy extraction.
Multi-MPPT inverter: A type of inverter with multiple Maximum Power Point Trackers (MPPTs), allowing for independent optimization of different PV module strings.
Central inverter: A high-capacity inverter that converts DC from multiple PV strings into AC. Common in large-scale PV systems, it offers cost efficiency but is prone to energy losses due to shading and module mismatch.
Micro-inverter: A small inverter attached to each PV module, converting DC to AC at the module level. It enhances energy yield, mitigates shading effects, and allows individual module monitoring but is costlier than central inverters.
East-West (E-W) Orientation: A PV panel configuration where modules are installed facing east and west, designed to extend the energy generation window throughout the day.
Shading effect: The reduction in energy output due to partial or complete obstruction of sunlight on PV panels.
Temperature-corrected Performance Ratio (PRT): A modified PR metric that accounts for temperature variations affecting PV efficiency.
Rated power (P_0): The rated power output of a PV system under standard test conditions.
Nominal connection capacity (P_{des}): Nominal or design connection capacity between the system and the electrical grid.
Tilt angle: The angle between a PV panel and the horizontal plane, which affects solar energy capture and varies depending on geographic location.
Photovoltaic degradation rate: The gradual decline in PV module performance over time, typically expressed as a percentage loss per year.